

Journal Pre-proof

Design, synthesis and biological evaluation of novel *N*-[4-(2-fluorophenoxy)pyridin-2-yl]cyclopropanecarboxamide derivatives as potential c-Met kinase inhibitors

Ju Liu, Yilin Gong, Jiantao Shi, Xuechen Hao, Yang Wang, Yunpeng Zhou, Yunlei Hou, Yajing Liu, Shi Ding, Ye Chen



PII: S0223-5234(20)30211-7

DOI: <https://doi.org/10.1016/j.ejmech.2020.112244>

Reference: EJMECH 112244

To appear in: *European Journal of Medicinal Chemistry*

Received Date: 28 December 2019

Revised Date: 8 March 2020

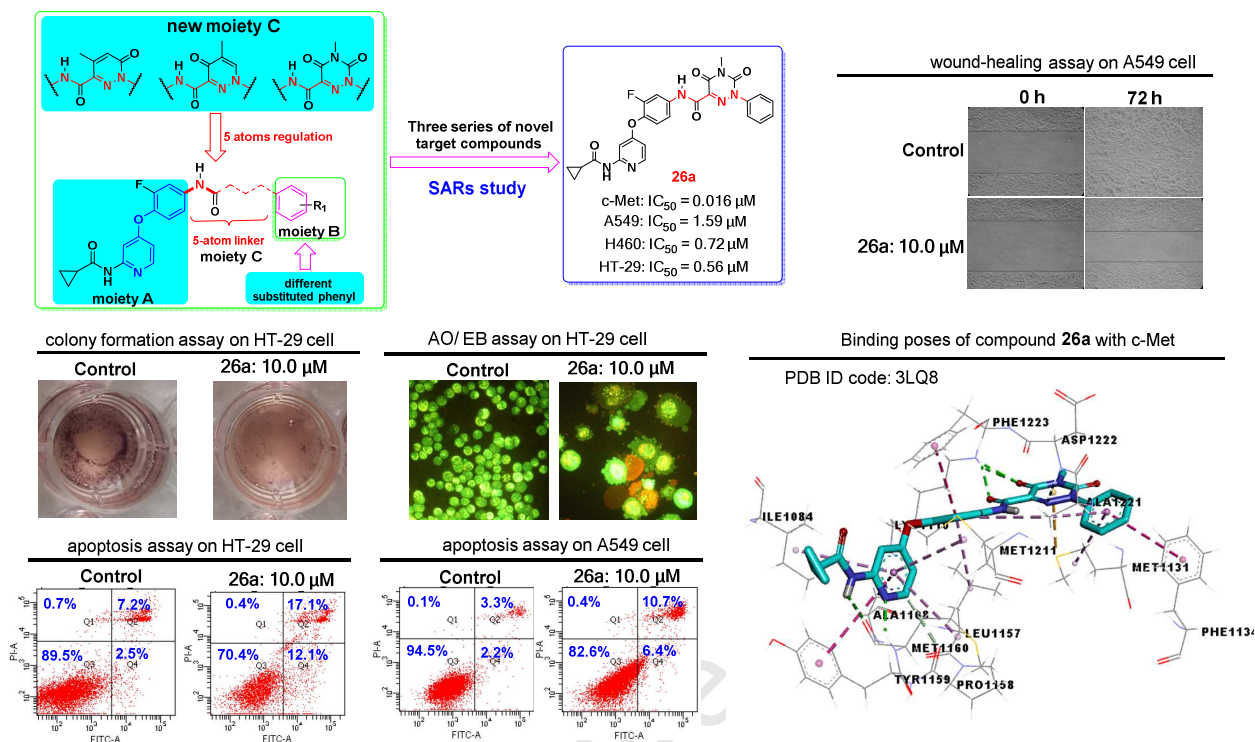
Accepted Date: 16 March 2020

Please cite this article as: J. Liu, Y. Gong, J. Shi, X. Hao, Y. Wang, Y. Zhou, Y. Hou, Y. Liu, S. Ding, Y. Chen, Design, synthesis and biological evaluation of novel *N*-[4-(2-fluorophenoxy)pyridin-2-yl]cyclopropanecarboxamide derivatives as potential c-Met kinase inhibitors, *European Journal of Medicinal Chemistry* (2020), doi: <https://doi.org/10.1016/j.ejmech.2020.112244>.

This is a PDF file of an article that has undergone enhancements after acceptance, such as the addition of a cover page and metadata, and formatting for readability, but it is not yet the definitive version of record. This version will undergo additional copyediting, typesetting and review before it is published in its final form, but we are providing this version to give early visibility of the article. Please note that, during the production process, errors may be discovered which could affect the content, and all legal disclaimers that apply to the journal pertain.

© 2020 Published by Elsevier Masson SAS.

Graphical abstract



Three series of novel 4-phenoxy-pyridine derivatives were synthesized and evaluated for their c-Met kinase activities and cytotoxic activities against A549, H460, HT-29 cancer cell lines. Furthermore, colony formation, acridine orange/ethidium bromide staining, apoptosis, and wound-healing assay of **26a** were performed.

Design, synthesis and biological evaluation of novel *N*-[4-(2-fluorophenoxy)pyridin-2-yl]cyclopropanecarboxamide derivatives as potential c-Met kinase inhibitors

Ju Liu^a, Yilin Gong^a, Jiantao Shi^a, Xuechen Hao^a, Yang Wang^a, Yunpeng Zhou^a,

Yunlei Hou^b, Yajing Liu^b, Shi Ding^{a,*}, Ye Chen^{a,**}

^a College of Pharmacy of Liaoning University, API Engineering Technology Research Center of Liaoning Province, 66 Chongshan Road, Huanggu District, Shenyang 10036, P. R. China.

^b Key Laboratory of Structure-Based Drug Design and Discovery (Shenyang Pharmaceutical University), Ministry of Education, 103 Wenhua Road, Shenhe District, Shenyang 110016, PR China

*Corresponding author: Shi Ding. Tel./Fax: 86-24-6220 2469. E-mail: dingshi_destiny@163.com.

**Corresponding author: Ye Chen. Tel./Fax: 86-24-6220 2469. E-mail: sy-chenye@163.com.

Abstract

Three series of novel 4-phenoxy pyridine derivatives containing 4-methyl-6-oxo-1,6-dihydropyridazine-3-carboxamide, 5-methyl-4-oxo-1,4-dihydropyridazine-3-carboxamide and 4-methyl-3,5-dioxo-2,3,4,5-tetrahydro-1,2,4-triazine-6-carboxamide moieties were synthesized and evaluated for their *in vitro* inhibitory activities against c-Met kinase and cytotoxic activities against A549, H460, HT-29 cancer cell lines. The results indicated that most of the compounds showed moderate to good antitumor activities. The most promising compound **26a** (with c-Met IC₅₀ value of 0.016 μM) showed remarkable cytotoxicity against A549, H460, and HT-29 cell lines with IC₅₀ values of 1.59 μM, 0.72 μM and 0.56 μM, respectively. Their preliminary structure-activity relationships (SARs) studies indicate that 4-methyl-3,5-dioxo-2,3,4,5-tetrahydro-1,2,4-triazine-6-carboxamide was more preferred as linker part, and electron-withdrawing groups on the terminal phenyl rings are beneficial for improving the antitumor activities. Furthermore, the colony formation, acridine orange/ethidium bromide (AO/EB) staining, apoptosis, and wound-healing assay of **26a** were performed on HT-29 and/or A549 cell lines.

Keywords: Synthesis, 4-Phenoxy pyridine derivatives, c-Met inhibitors, Antitumor activity, Docking study.

1. Introduction

c-Mesenchymal epithelial transition factor (c-Met) is a receptor tyrosine kinase that is normally activated by its natural ligand hepatocyte growth factor/scatter factor (HGF/SF) [1]. The HGF/c-Met axis plays an important role in normal embryonic development and organ regeneration. However, aberrant activation of c-Met can increase the tumorigenicity and metastatic potential of tumor cells [2]. Like other oncogenic pathway, overexpression or mutation of protein members of this pathway is a driving factor for numerous cancers [3]. Consequently, the HGF/c-Met signaling pathway has been emerging as an attractive target for cancer therapies [4].

To date, numerous examples of successful therapeutic interventions with small molecule c-Met kinase inhibitors have been reported [5]. These small molecule c-Met kinase inhibitors were mainly divided into Type I and Type II, according to the structural features and binding mode to the c-Met kinase. As disclosed recently, certain mutations near the active site of c-Met may cause resistance of type I inhibitors. In contrast, type II inhibitors are postulated to be more effective against these mutations because their binding interactions extend beyond the entrance to c-Met's active site [6-8]. During the past ten years, numerous type II c-Met inhibitors have been discovered and some of them are launched or in clinical trials, such as Cabozantinib [9], BMS-777607 [10], BMS-794833 [11], Foretinib [12] and NPS-1034 [13] (Fig. 1). Among them, 4-phenoxy pyridines play a key role and have been extensively studied [14-18]. A good example of 4-phenoxy pyridine-based type II c-Met inhibitors is BMS-777607,

which inhibits the kinase activity of c-Met ($IC_{50} = 3.9$ nM), as well as that of Axl ($IC_{50} = 1.1$ nM), Ron ($IC_{50} = 1.8$ nM), and Tyro3 ($IC_{50} = 4.3$ nM), is currently undergoing phase II clinical trials for various cancers [10].

As described in Fig. 1, structurally, most of type II c-Met inhibitors may be disconnected into three moieties: a 4-phenoxy pyridine core (moiety A, usually substituted 4-phenoxy pyridine, 4-phenoxyquinoline, 4-phenoxy pyrrolopyridine, and 4-phenoxy thienopyridine), a phenyl or substituted phenyl group (moiety B) and a linker bridge (moiety C). Importantly, there should be two structural characteristics on the linker bridge (moiety C) between moiety A and B. One was '5-atom regulation', which means six chemical bonds distance existing between moiety A and B; the other was that the linker should contain both hydrogen-bond donor or acceptor and at least one amide group. Various linear chains and heterocyclic rings can be introduced to the main chain of 5-atom linker [19-21].

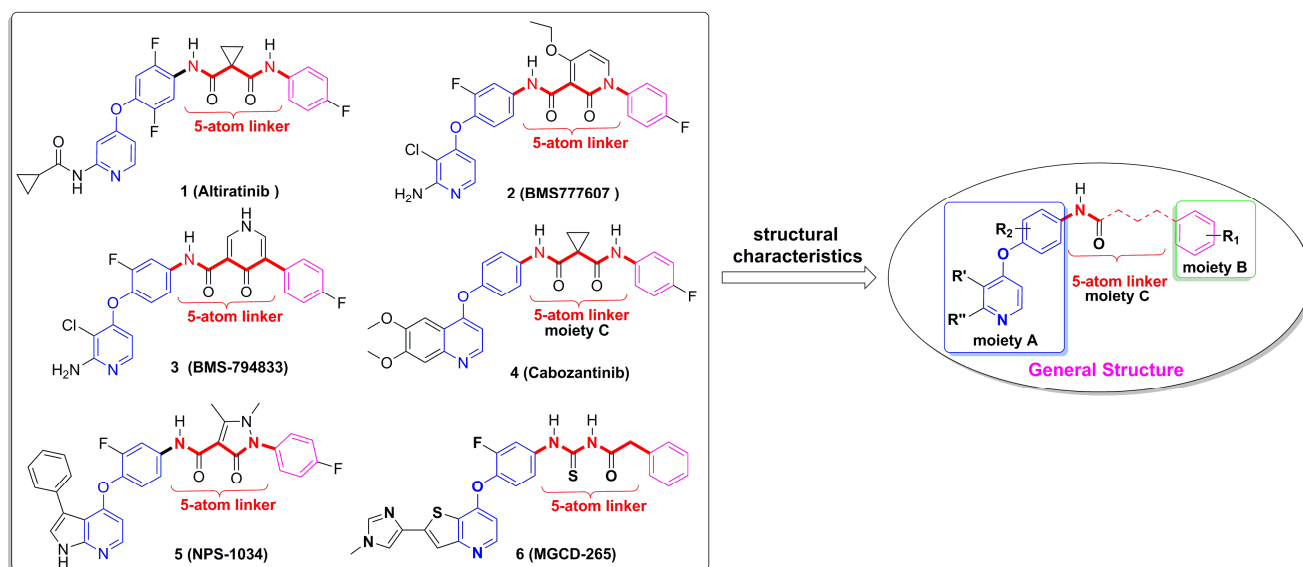


Fig. 1. The representative c-Met kinase inhibitors and the corresponding general structure.

With the goal of finding more 4-phenoxy pyridine-based type II c-Met inhibitors, *N*-[4-(2-fluorophenoxy)pyridin-2-yl]cyclopropanecarboxamide was used as the moiety A. 4-Methyl-6-oxo-1,6-dihydropyridazine-3-carboxamide, 5-methyl-4-oxo-1,4-dihydropyridazine-3-carboxamide and 4-methyl-3,5-dioxo-2,3,4,5-tetrahydro-1,2,4-triazine-6-carboxamide fragments were introduced into the moiety C via cyclization strategy based on the '5 atoms regulation'. Furthermore, various substituents were introduced at the phenyl ring (moiety B) to investigate their effects on activities. Accordingly, three series of 4-phenoxy pyridine derivatives were designed and synthesized to study the structure-activity relationships (SARs) and find promising antitumor agents (Fig. 2).

In the current study, all target compounds were synthesized and evaluated for their *in vitro* inhibitory activities against c-Met kinase and cytotoxic activities against human lung adenocarcinoma cell line (A549), human lung cancer cell lines (H460) and human colon cancer cell line (HT-29) cancer cell lines. Their structure-activity relationships (SARs) were further explored. Furthermore, the colony formation, acridine orange/ethidium bromide (AO/EB) staining, apoptosis, and wound-healing assays of **26a** were performed on HT-29 and/or A549 cell lines. Additionally, a docking analysis was also performed to elucidate the binding mode of the target compound **26a** with c-Met kinase.

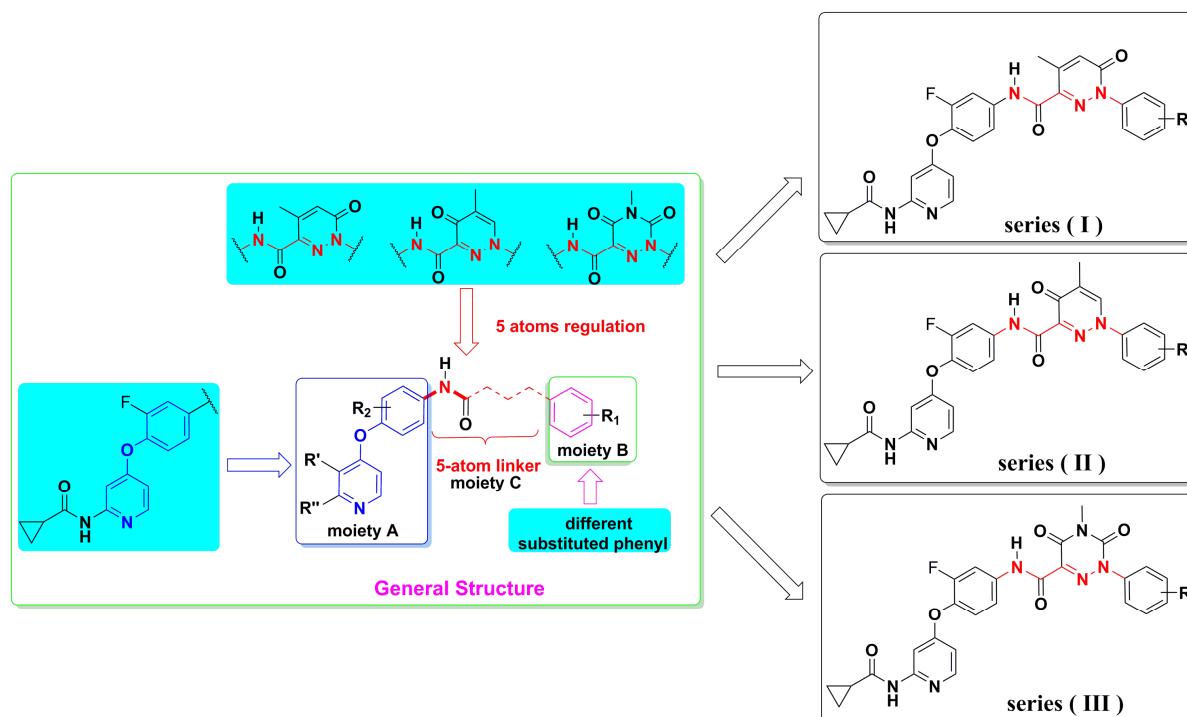
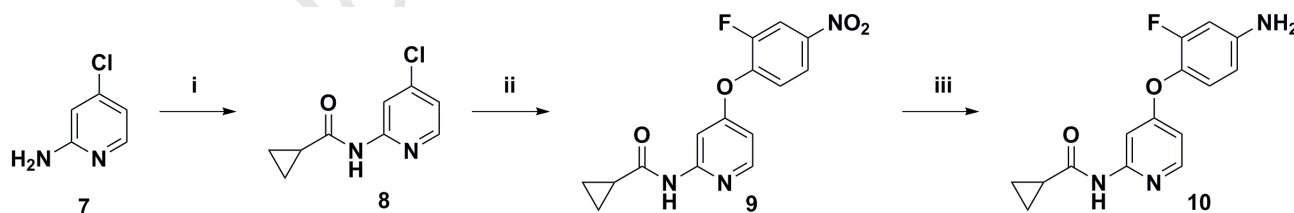


Fig. 2. Design strategy and structures of the target compounds.

2. Results and discussion

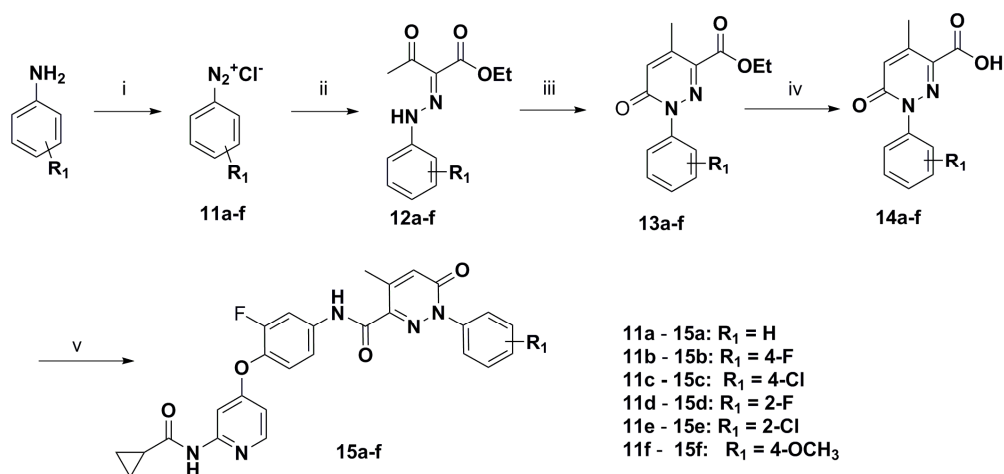
2.1 Chemistry

The key intermediate **10** was synthesized according to the route outlined in Scheme 1. Commercially available 4-chloropyridin-2-amine was condensed with cyclopropanecarbonyl chloride in the presence of Et_3N to provide **8**, which underwent a nucleophilic substitution with 2-fluoro-4-nitrophenol to give the desired intermediate **9**. Reduction of the nitro group of **9** with iron powder and acetic acid in ethyl acetate /water (10:1 v/v) provided aniline compound **10**.



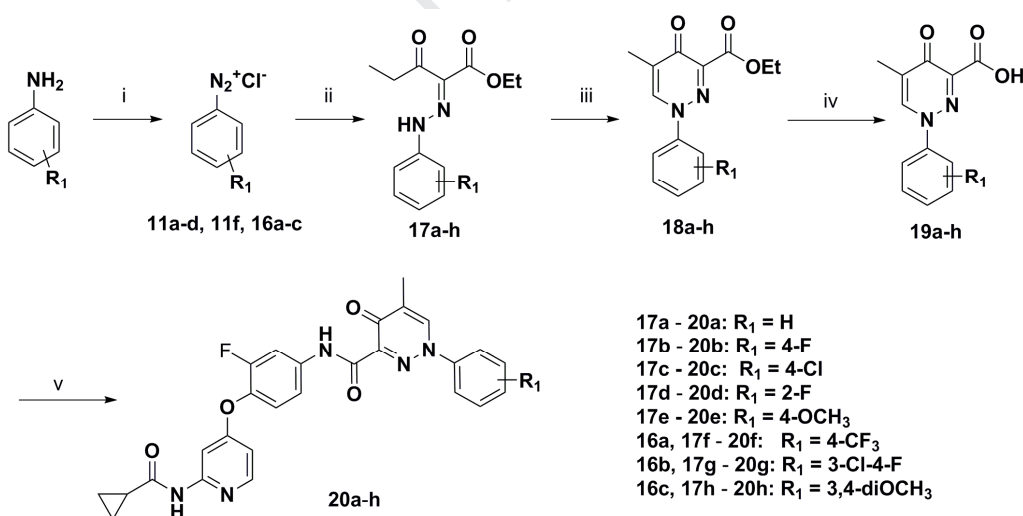
Scheme 1. Reagents and conditions: (i) cyclopropanecarbonyl chloride, Et_3N , CH_2Cl_2 , rt, 12 h; (ii) 2-fluoro-4-nitrophenol, chlorobenzene, reflux, 40 h; (iii) Fe (powder), HOAc, ethyl acetate /water (5:1 v/v), reflux, 2 h.

The synthesis of target compounds **15a-f** were summarized in Scheme 2. The condensation of commercially available ethyl acetoacetate with different substituted diazotized anilines in the presence of sodium acetate in ethanol/water mixture afforded intermediates **12a-f** as yellow solids. The cyclization of **12a-f** with (ethoxycarbonylmethylene)triphenylphosphorane in refluxing toluene gave compounds **13a-f**, which were converted to acids **14a-f** using sodium hydroxide solution at 50 °C for 5 h [22, 23]. Acids **14a-f** were then condensed with intermediate **10** in the presence of HATU and Et_3N in DMF at room temperature overnight to afford the target compounds **15a-f**.



Scheme 2. Reagents and conditions: (i) NaNO₂, HCl, H₂O, 0 °C, 30 min; (ii) Ethyl acetoacetate, AcONa, EtOH, 0-25 °C, 2 h; (iii) Ph₃P=CHCOOEt, PhMe, reflux, 12 h; (iv) NaOH, THF / H₂O, 50 °C, 5 h; (v) **10**, HATU, Et₃N, DMF, rt, 12 h.

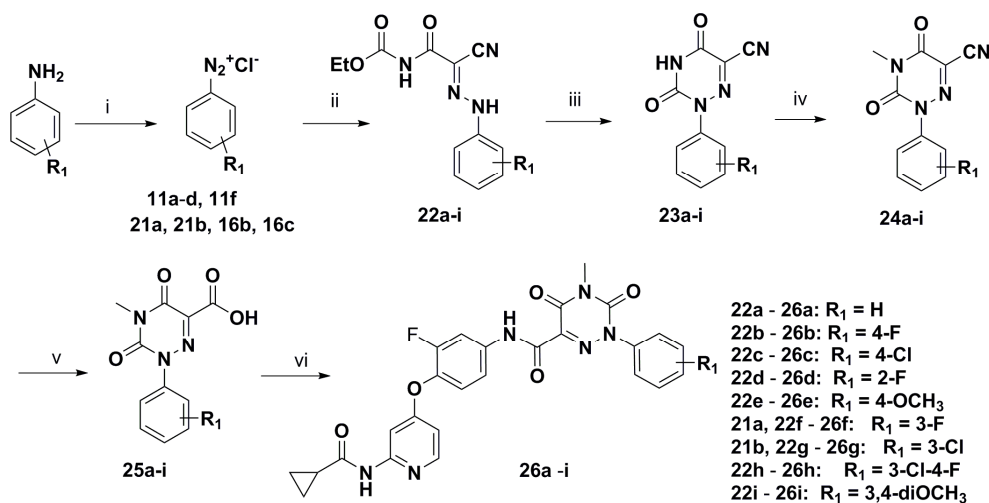
The target compounds **20a-h** were synthesized according to the method summarized in Scheme 3. According to the similar synthesis procedure of **12a-h**, diazotization of the substituted anilines with sodium nitrite in aqueous hydrochloric acid, followed by condensation with ethyl 3-oxopentanoate in basic medium afforded the corresponding intermediates **17a-h** in good to excellent yields. The cyclization of **17a-h** with DMF-DMA afforded 1-aryl-4-oxo-1,4-dihydropyridazine-3-carboxylic acid esters **18a-h**, which were converted to acid analogues **19a-h** by hydrolysis in aqueous NaOH [24]. Finally, intermediates **19a-h** were coupled with intermediate **10** using HATU as coupling reactant to afford the target compounds **20a-h**.



Scheme 3. Reagents and conditions: (i) NaNO₂, HCl, H₂O, 0 °C, 30 min; (ii) ethyl 3-oxopentanoate, AcONa, EtOH, 0-25 °C, 2 h; (iii) DMF-DMA, PhMe, reflux, 12 h; (iv) 10% NaOH, 50 °C, 4 h; (v) **10**, HATU, Et₃N, DMF, rt, 12 h.

The target compounds **26a-i** were obtained using a five-step synthetic route outlined in Scheme 4. Ethyl (2-cyanoacetyl)carbamate was added to a freshly synthesized different substituted phenyl diazonium chloride, obtained by action of sodium nitrite on substituted aniline hydrochloride, in the presence of sodium acetate in ethanol to give the ethyl [2-cyano-2-(2-arylhydrazono)acetyl]carbamate derivative **22a-i**, which were converted into analogues **23a-i** by intramolecular cyclization in the presence of sodium acetate in refluxed acetic acid. *N*-methylation of **23a-i** with iodomethane in anhydrous DMF, in the presence of sodium hydride, gave the desired intermediates **24a-i**, which were hydrolyzed with acetic acid and hydrochloric acid gave rise to carboxylic acid

derivatives **25a-i** [15, 25]. Coupling reaction of **25a-i** with intermediate **10** produced the corresponding target compounds **26a-i** in the presence of HATU and Et₃N in DMF at room temperature.



Scheme 4. Reagents and conditions: (i) NaNO₂, HCl, H₂O, 0 °C, 30 min; (ii) ethyl (2-cyanoacetyl)carbamate, AcONa, EtOH, 0 °C, 2 h; (iii) HOAc, AcONa, reflux, 2 h; (iv) NaH, CH₃I, DMF, 0 °C, then rt, 5 h; (v) HOAc, HCl, H₂O, reflux, 4 h; (vi) **10**, HATU, Et₃N, DMF, rt, 12 h.

2.2 Biological evaluation

2.2.1 *In vitro* c-Met kinase assays and analysis of the structure-activity relationships

All the newly synthesized 4-phenoxy pyridine derivatives (**15a-f**, **20a-h**, and **26a-i**) were evaluated for their *in vitro* inhibitory activity toward c-Met kinase using mobility shift assay. Foretinib was used as a positive control, with the results expressed as half-maximal inhibitory concentration (IC₅₀) values presented in Table 1. The IC₅₀ values are the average of at least three independent experiments.

As illustrated in Table 1, all the tested compounds showed moderate to excellent c-Met kinase activity with IC₅₀ values ranging from 0.016 to 3.54 μM, which indicated that introduction of the 4-methyl-3,5-dioxo-2,3,4,5-tetrahydro-1,2,4-triazine-6-carboxamide, 5-methyl-4-oxo-1,4-dihydropyridazine-3-carboxamide or 4-methyl-6-oxo-1,6-dihydropyridazine-3-carboxamide framework to “**5-atom linker**” moiety of pyridine-based c-Met kinase inhibitor maintained the c-Met inhibitory efficacy. Notably, Nine of them (**20a-d**, **26a-d**, **26f**, **26g**) exhibited promising activity against c-Met kinase with IC₅₀ values less than 0.10 μM, and compound **26a** demonstrated the best activity with an IC₅₀ value of 0.016 μM.

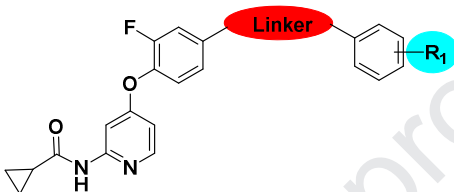
The structure-activity relationship (SAR) was commenced by the introduction of “**5-atom linker**” that contains different kinds of nitrogen aromatic heterocyclic between moiety A and moiety B. Based on the pharmacological data in Table 1, we could deduce that different “**5-atom linker**” had a marked influence on c-Met kinase potency with the following rank order generally: 4-methyl-3,5-dioxo-2,3,4,5-tetrahydro-1,2,4-triazine-6-carboxamide > 5-methyl-4-oxo-1,4-dihydropyridazine-3-carboxamide > 4-methyl-6-oxo-1,6-dihydropyridazine-3-carboxamide. For example, the activity of compound **26b** (IC₅₀ = 0.031 μM, R = 4-F) was higher than compound **20b** (IC₅₀ = 0.044 μM, R = 4-F) and compound **15b** (IC₅₀ = 0.15 μM, R = 4-F), which suggested 4-methyl-3,5-dioxo-2,3,4,5-tetrahydro-1,2,4-triazine-6-carboxamide was more preferred.

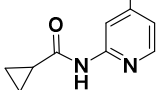
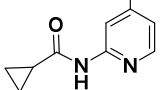
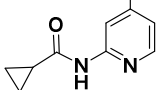
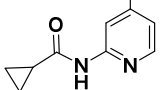
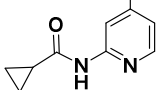
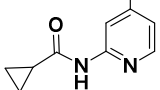
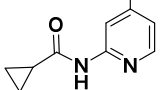
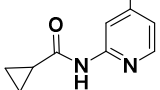
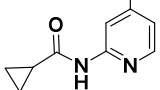
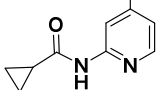
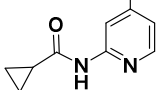
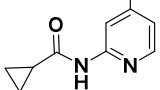
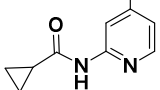
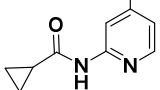
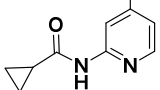
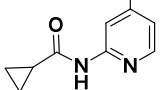
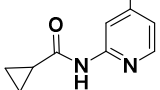
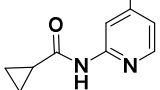
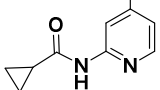
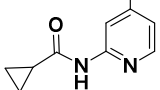
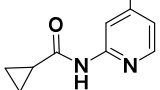
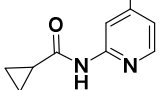
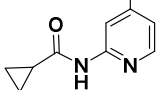
Further analysis revealed that compounds with the same “**5-atom linker**” but different substituents on the terminal phenyl ring (moiety B) showed different c-Met inhibitory efficacy. Introduction of mono-electron-withdrawing groups (mono-EWGs), especially halogen groups, on the phenyl ring led to a positive effect in activity, such as compounds **20c** (R = 4-Cl, IC₅₀ = 0.057 μM) and **26b** (R = 4-F, IC₅₀ = 0.031 μM). However,

strong-withdrawing groups and double-electron-withdrawing groups (double-EWGs) and mono-electron-donating groups (mono-EDGs) exhibited a negative effect compared to no substituent on the phenyl ring, such as compound **20f** (R = 4-CF₃, IC₅₀ = 0.24 μM), compound **26h** (R = 3-Cl-4-F, IC₅₀ = 0.37 μM) and **20e** (R = 4-OCH₃, IC₅₀ = 0.28 μM). Incorporation of double-electron-donating groups (double-EDGs) such as 3, 4-dimethoxy analogue (**20h**: IC₅₀ = 3.54 μM; **26i**: IC₅₀ = 2.08 μM) lowered the efficiency even further. Moreover, it was worth noting that the position of R group was closely related to c-Met inhibitory efficiency as well. Compounds with 4-substituted phenyl group (**15b**, R = 4-F, IC₅₀ = 0.15 μM; **20b**, R = 4-F, IC₅₀ = 0.044 μM; **26c**, R = 4-Cl, IC₅₀ = 0.046 μM) displayed higher potency than those with 2-substituted phenyl group (**15d**, R = 2-F, IC₅₀ = 0.88 μM; **20d**, R = 2-F, IC₅₀ = 0.062 μM) or 3-substituted phenyl group (**26g**, R = 3-Cl, IC₅₀ = 0.098 μM).

Table 1

Cytotoxicity of target compounds against A549, H460 and HT-29 cells and c-Met kinase inhibition *in vitro*.



Compd.	Linker	R ₁	IC ₅₀ (μM) ± SD ^a			
			c-Met	A549	H460	HT-29
15a		H	0.35 ± 0.04	4.85 ± 0.33	4.30 ± 0.27	2.93 ± 0.21
15b		4-F	0.15 ± 0.02	3.07 ± 0.24	2.61 ± 0.14	3.94 ± 0.26
15c		4-Cl	0.23 ± 0.05	6.38 ± 0.72	3.49 ± 0.31	2.07 ± 0.17
15d		2-F	0.88 ± 0.10	4.64 ± 0.41	5.84 ± 0.49	4.11 ± 0.30
15e		2-Cl	1.05 ± 0.09	5.47 ± 0.38	2.62 ± 0.09	4.47 ± 0.22
15f		4-OCH ₃	2.72 ± 0.13	10.56 ± 0.73	13.09 ± 0.96	8.36 ± 0.61
20a		H	0.076 ± 0.004	4.67 ± 0.16	2.85 ± 0.15	1.56 ± 0.08
20b		4-F	0.044 ± 0.007	1.82 ± 0.12	0.79 ± 0.09	1.43 ± 0.10
20c		4-Cl	0.057 ± 0.005	6.74 ± 0.44	2.23 ± 0.12	0.63 ± 0.04
20d		2-F	0.062 ± 0.008	2.79 ± 0.11	1.83 ± 0.14	2.31 ± 0.18
20e		4-OCH ₃	0.28 ± 0.04	7.91 ± 0.64	17.16 ± 1.08	5.35 ± 0.13
20f		4-CF ₃	0.24 ± 0.06	6.84 ± 0.50	7.45 ± 0.52	2.92 ± 0.27
20g		3-Cl-4-F	0.47 ± 0.09	4.64 ± 0.37	3.89 ± 0.25	7.83 ± 0.56
20h		3,4-diOCH ₃	3.54 ± 0.37	8.75 ± 0.46	5.26 ± 0.31	9.87 ± 0.72
26a		H	0.016 ± 0.002	1.59 ± 0.09	0.72 ± 0.05	0.56 ± 0.04
26b		4-F	0.031 ± 0.004	3.42 ± 0.16	0.64 ± 0.06	1.03 ± 0.08
26c		4-Cl	0.046 ± 0.006	3.02 ± 0.25	1.19 ± 0.11	0.83 ± 0.07
26d		2-F	0.058 ± 0.008	2.56 ± 0.13	1.37 ± 0.13	2.46 ± 0.16
26e		4-OCH ₃	0.94 ± 0.07	5.86 ± 0.59	6.56 ± 0.46	2.69 ± 0.13
26f		3-F	0.073 ± 0.003	2.13 ± 0.18	3.01 ± 0.18	1.63 ± 0.11
26g		3-Cl	0.098 ± 0.005	4.18 ± 0.37	1.96 ± 0.14	2.43 ± 0.20
26h		3-Cl-4-F	0.37 ± 0.09	4.67 ± 0.29	3.36 ± 0.27	4.61 ± 0.38
26i		3,4-diOCH ₃	2.08 ± 0.19	6.18 ± 0.45	7.94 ± 0.66	3.78 ± 0.23
Foretinib ^b	--	--	0.004 ± 0.0003	1.05 ± 0.08	0.81 ± 0.05	0.98 ± 0.07

^a Data presented is the mean ± SD value of three independent determinations.

^b Used as a positive control.

2.2.2 *In vitro* antiproliferative activity

All the target compounds were further evaluated for their antitumor activities against three c-Met overexpressed human cancer cell lines, namely A549 (human lung adenocarcinoma cell line), H460 (human lung cancer cell line) and HT-29 (human colon cancer cell line) together with foretinib as the positive control by a MTT assay. The data listed in Table 1 revealed that all the target compounds (**15a-f**, **20a-h**, and **26a-i**) possessed moderate to strong cytotoxicity against the three tested cell lines, and high selectivity for of inhibition H460 and HT29 cells, and five of them were more potent than foretinib against one or more cell lines. Among them, compound **26a** exhibited remarkable inhibitory activity against H460 and HT-29 cell lines with IC_{50} value of 0.72 and 0.56 μ M, respectively, which were more potent than that of the positive control foretinib (IC_{50} = 0.81 μ M and 0.98 μ M). The cytotoxic activities of these compounds showed similar structure–activity relationships (SARs) with summarized in the c-Met kinase level: (a) compounds with 4-methyl-3,5-dioxo-2,3,4,5-tetrahydro-1,2,4-triazine-6-carboxamide as “5-atom linker” exhibited strong cytotoxicity than the other two linkers (b) compounds bearing mono-EWGs on the phenyl ring(F or Cl) were generally more active than those with double-EWGs or EDGs; (d) the cytotoxicity of compounds with substituent at 4-position of phenyl ring were higher than those with substituents at other positions.

2.2.3. Colony formation inhibition ability of **26a**

Colony formation assay is commonly used to determine longterm effects of cytotoxic agents on cancer cell growth *in vitro*. Colony formation assay can be used not only to measure direct immediate impact of compounds on cancer cells but also to estimate anti-proliferative potency or long-term recurrence prevention efficacy of compounds [26]. According to the results of MTT, *in vitro* clonogenic assay was performed to measure the cell proliferation capability *i.e.* the ability of a single cell to grow into a colony. This assay tests each and every cell in the population for its ability to undergo unlimited divisions [27]. Based on the most excellent activity against HT-29 cells, cell proliferation inhibiting ability of compound **26a** was measured using colony formation assay. The results from the Fig. 3 showed that the colony formation efficiency from 25.3 ± 1.21 % in control decreased to 12.2 ± 1.27 % at 1.0 μ M and 4.8 ± 0.45 % at 10.0 μ M, respectively. These experiments indicated that compound **26a** suppressed the colony formation and inhibited the unrestricted growth of HT-29 cancer cells in a concentration-dependent manner.

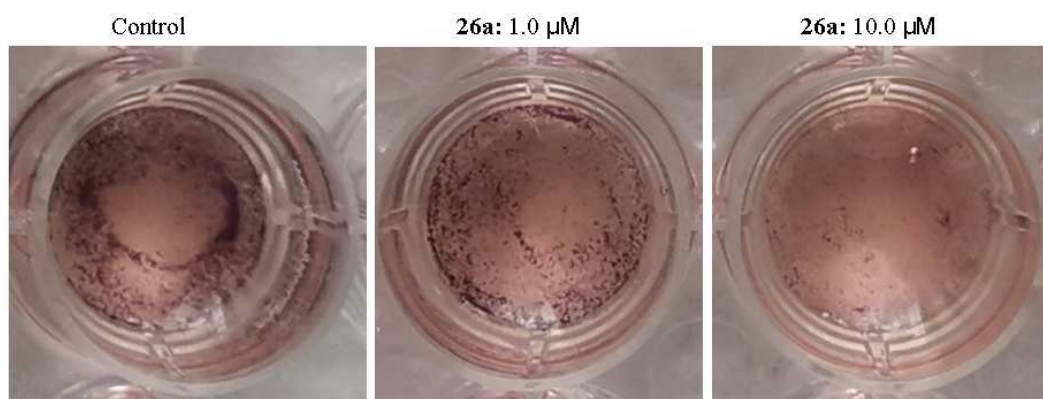


Fig. 3. Various concentrations of compound **26a** inhibited colony formation of HT-29 cells for 7 days.

2.2.4. Apoptosis induction ability of **26a**

Compound **26a** was further confirmed by an acridine orange (AO)/ethidium bromide (EB) assay to examine the occurrence of apoptosis in HT-29 cells. EB was able to penetrate through intact membranes of live cells and colors DNA as green fluorescence, while AO was only taken up by apoptotic cells with damaged membranes coloring DNA as orange fluorescence. Therefore, normal live cells appeared uniformly stained green in color. Early apoptotic cells contained bright green condensed bodies in their nuclei representing nuclear DNA fragmentation and later apoptotic cells presented colored orange nuclei indicating that their membranes are broken [28, 29]. It can be

inferred from Fig.4 that the control cells showed normal morphology and appeared green in color. Fluorescence microscopic images of cells treated with 1.0 μM and 10.0 μM of compound **26a** clearly showed the morphological changes such as cell shrinkage, membrane blebbing, chromatin condensation and apoptotic body formation, suggesting that compound **26a** induced dose-dependent cell death in HT-29 cancer cells *via* apoptosis.

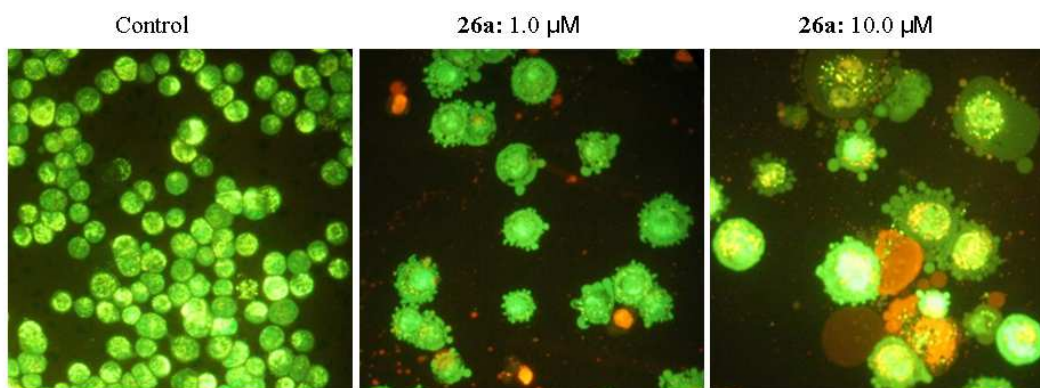


Fig. 4. AO/EB stained apoptosis of HT-29 cell lines with different concentrations of compound **26a** for 48 h.

Subsequently, apoptosis was measured by Annexin V/PI double staining by flow cytometry to quantify the percentage of cells undergoing apoptosis by compound **26a** according to known procedures [30]. This assay facilitates the detection of live cells, early apoptotic cells, late apoptotic cells and necrotic cells. HT-29 and A549 cells were seeded per well in six-well plates and were treated with compound **26a** of different concentrations (0, 1.0 and 10.0 μM) for 48 h, respectively. The result was shown in Fig. 5. The upper right section represents the cells which were in the late apoptotic cells, and the lower right section represents the early or middle apoptosis. Results from the Fig. 5 indicated that the percentage of total apoptotic cells (early and late apoptotic cells) from 9.7% (control) increased to 15.8 % at 1.0 μM , 29.2 % at 10.0 μM , in HT-29 cells, and the same trend was observed in A549 cells. The increase of total apoptotic cells indicated that compound **26a** induced apoptosis in HT-29 and A549 cells in a dose dependent manner.

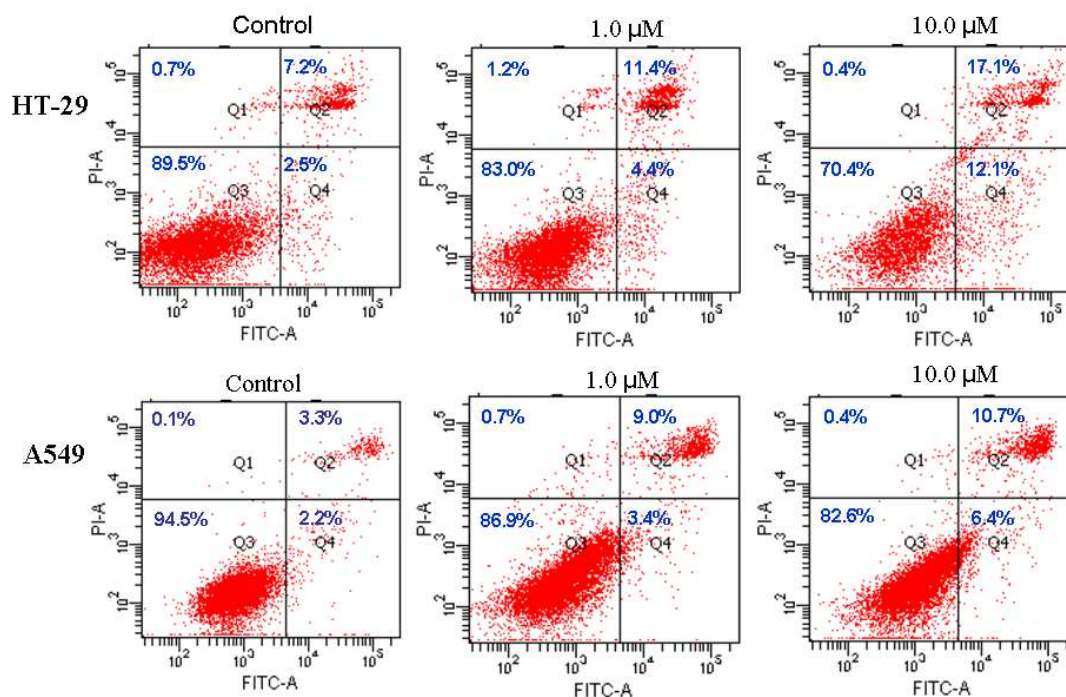


Fig. 5. Compound **26a** induces cell apoptosis of HT-29 and A549 cell line *in vitro*.

2.2.5. Cell migration inhibition ability of **26a**

Cell migration is a highly coordinated and multi-step process that plays a critical role in progression of cancer. Cancer cells often have a highly metastatic nature. Wound-healing assay is a simple and inexpensive method to study the directional migration of cells *in vitro* [31]. Thus, we investigated the antimigratory effect of compound **26a** on A549 cells *in vitro* using wound-healing assay. As shown in Fig. 6, after 0, 12, 36 and 72 h at 0 and 1.0 μM study revealed that compound **26a** was sufficient to block the movement of most A549 cells at a dose of 1.0 μM compared to the control. These results indicated that compound **26a** strongly inhibited A549 cell motility.

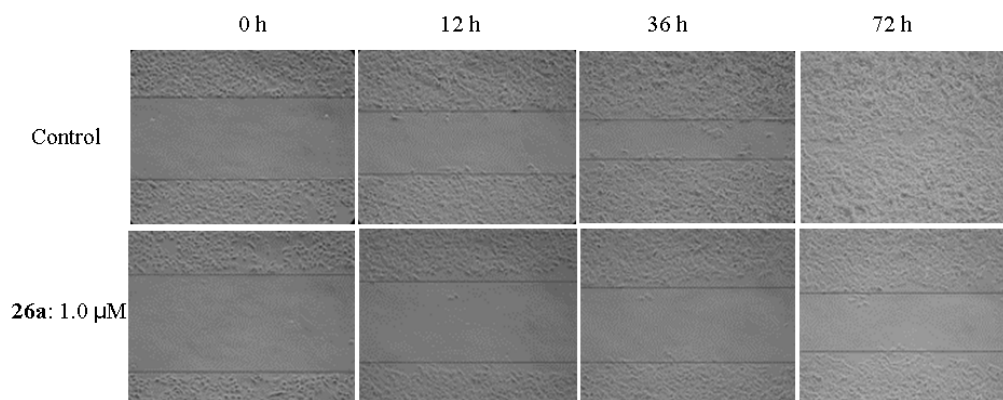


Fig. 6. Effect of compound **26a** *in vitro* migration potential of A549 cells.

2.2.6. Binding mode analysis

To further elucidate the binding mode of compounds, a detail docking analysis was performed. In our study, the co-crystal structure of foretinib (GSK1363089) with c-Met was selected as the docking model (PDB ID code: 3LQ8). The docking simulation was conducted using Glide XP (Schrödinger 2014), since Glide uses a hierarchical series of filters to search for possible locations of the ligand in the active-site region of the receptor. The shape and properties of the receptor are represented on a grid by several different sets of fields that provide progressively more accurate scoring of the ligand poses. The image files were generated using Accelrys DS visualizer 4.0 system. The binding mode was exemplified by the interaction of compound **26a** with c-Met. As shown in Fig. 7, the N atom of pyridine and the NH of cyclopropanecarboxamide interacted with Met1160 *via* two hydrogen bonds, and the 4-methyl-3,5-dioxo-2,3,4,5-tetrahydro-1,2,4-triazine-6-carboxamide moiety formed three hydrogen bonds with Asp1222 and Lys1110, respectively. Meanwhile, pyridyl ring, the phenyl ring at 4-position of pyridine and the phenyl ring at 1-position of triazine formed three π - π interactions with Tyr1159, Phe1223 and Phe1134, respectively. All these interactions contribute to the tight binding and greatly enhance the inhibitory potency of **26a**.

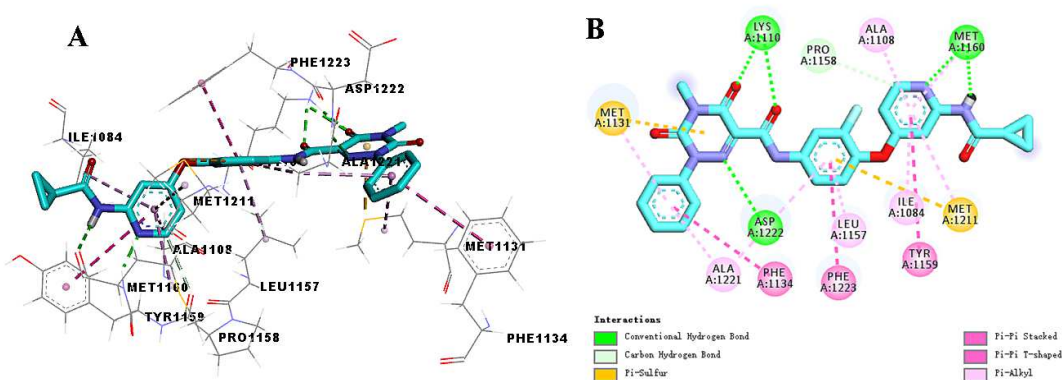


Fig. 7. Binding poses of compound **26a** with c-Met (A); 2D interactions of the docking model of **26a** to c-Met (B)

3. Conclusion

In summary, twenty-three novel 4-phenoxy pyridine derivatives containing 4-methyl-6-oxo-1,6-dihydropyridazine-3-carboxamide, 5-methyl-4-oxo-1,4-dihydropyridazine-3-carboxamide and 4-methyl-3,5-dioxo-2,3,4,5-tetrahydro-1,2,4-triazine-6-carboxamide moieties as c-Met inhibitors were designed, synthesized and evaluated for their biological activities. The screening of c-Met kinase activities and cytotoxicity led to the identification of a most promising compound **26a** (c-Met IC₅₀ = 0.016 μM) with IC₅₀ values of 1.59 μM, 0.72 μM and 0.56 μM against A549, H460, and HT-29 cells, representing a promising lead for further optimization. The initial SARs analysis disclosed that the 4-methyl-3,5-dioxo-2,3,4,5-tetrahydro-1,2,4-triazine-6-carboxamide scaffold was more preferred as linker part, and electron-withdrawing groups on the terminal phenyl rings are beneficial for improving the antitumor activities. Meanwhile, colony formation assays, AO/EB assays, cell apoptosis assays by flow cytometry, and wound-healing assays on HT-29 and/or A549 cells results indicated that compound **26a** could suppress the colony formation on HT-29 cells, induce HT-29 and A549 cells apoptosis, and inhibit A549 cells motility. Further studies on structural optimization and biological activities about these derivatives are still underway in our laboratory and will be reported in the future.

4. Experimental

4.1. Chemistry

Unless otherwise specified, all melting points were obtained on a Beijing Taike X-4 microscopy melting point apparatus and were uncorrected. ¹H NMR spectra were recorded on a Bruker Biospin 600 MHz or Bruker Biospin 400 MHz instrument using TMS as the internal standard. All chemical shifts were reported in ppm. IR spectra were recorded as KBr pellets on a Perkin-Elmer Spectrum one FT-IR spectrometer. MS spectra were obtained on an Agilent 6460 QQQ mass spectrometer (Agilent, USA) analysis system. All materials were obtained from commercial suppliers and were used without further purification. Reactions' time and purity of the products were monitored by TLC on FLUKA silica gel aluminum cards (0.2 mm thickness) with fluorescent indicator 254 nm. Column chromatography was run on silica gel (200–300 mesh) from Qingdao Ocean Chemicals (Qingdao, Shandong, China). The key intermediates **11a-f**, **12a-f**, **13a-f** and **14a-f** were synthesized based on the previous literatures methods [22, 23]. The key intermediates **16a-c**, **17a-h**, **18a-h** and **19a-h** were synthesized according to our previous reported procedures [24]. The key intermediates **21a-b**, **22a-i**, **23a-i**, **24a-i** and **25a-i** were synthesized according to previous reported procedures [15, 25].

4.1.1. *N*-(4-Chloropyridin-2-yl)cyclopropanecarboxamide (**8**)

Cyclopropanecarbonyl chloride (9.30 g, 89.00 mmol) was dissolved in dried CH₂Cl₂ (30 mL) and drop-wise added to a mixture of 4-chloropyridin-2-amine (8.80 g, 68.45 mmol), Et₃N (20.78 g, 205.35 mmol) and CH₂Cl₂ (80 mL) in an ice bath, which was then removed to raise the temperature to room temperature and stirred for 12 h. The resulting mixture was sequentially washed with 20% K₂CO₃ (50 mL × 3) and brine (50 mL × 3), and the organic phase was separated, dried over anhydrous Na₂SO₄, filtered, and the filtrate was evaporated under reduced pressure. The crude product obtained was purified by silica gel chromatography to give 9.78 g (72.66%) of **13** as a white solid. IR (KBr) cm⁻¹: 3241.8 (NH), 1706.5 (C=O), 1670.1, 1588.4 (C=N), 1573.5, 1537.4, 1403.5; ¹H-NMR (400 MHz, DMSO-*d*₆) δ 11.04 (s, 1H), 8.30 (d, *J* = 5.2 Hz, 1H), 8.15 (s, 1H), 7.21 (d, *J* = 5.2 Hz, 1H), 2.00 (m, 1H), 0.85 (m, 4H); MS (ESI) *m/z*(%): 197.1 [M+H]⁺.

4.1.2. *N*-(4-(2-Fluoro-4-nitrophenoxy)pyridin-2-yl)cyclopropanecarboxamide (**9**)

A stirring mixture of compound **8** (8.00 g, 40.68 mmol) and 2-fluoro-4-nitrophenol (15.98 g, 101.71 mmol) in chlorobenzene (100 mL) was refluxed for about 40 h. After cooling to room temperature, the reaction mixture was

concentrated under reduced pressure to yield a pale solid. The solid was dissolved in CH₂Cl₂ (150 mL), and washed with saturated K₂CO₃ aqueous solution (80 mL × 4), then brine (60 mL × 4), and dried over anhydrous Na₂SO₄, concentrated under reduced pressure to afford a brown solid, which was purified by silica gel chromatography to give 7.13 g (55.24%) of **9** as a light yellow solid. IR (KBr) cm⁻¹: 3417.7 (NH), 1687.3 (C=O), 1616.7 (C=N), 1528.7 (C=C_{arom}), 1492.5 (C=C_{arom}); ¹H NMR (600 MHz, DMSO-*d*₆) δ 11.00 (s, 1H), 8.43 (dd, *J* = 10.3, 2.2 Hz, 1H), 8.30 (d, *J* = 5.7 Hz, 1H), 8.19 (dd, *J* = 9.0, 1.9 Hz, 1H), 7.76 (d, *J* = 2.2 Hz, 1H), 7.61 (t, *J* = 8.5 Hz, 1H), 6.86 (dd, *J* = 5.6, 2.2 Hz, 1H), 2.04 – 1.95 (m, 1H), 0.78 (t, *J* = 6.3 Hz, 4H); MS (ESI) *m/z*(%): 318.1 [M+H]⁺.

4.1.3. *N*-(4-(4-Amino-2-fluorophenoxy)pyridin-2-yl)cyclopropanecarboxamide (**10**)

A mixture of compound **9** (6.00 g, 18.91 mmol), iron powder (5.28 g, 94.56 mmol), acetic acid (11.36 g, 189.10 mmol), water (20 mL) and ethyl acetate (100 mL) was heated to reflux for 2 h. After completion of the reaction as indicated by TLC, the mixture was filtered immediately. The organic layer of the filtrate was separated, washed with water, dried over anhydrous Na₂SO₄, filtered, and the filtrate was evaporated under reduced pressure when white solid appeared, which was filtered to obtain 3.51 g (64.61%) of **10** as light yellow solid. IR (KBr) cm⁻¹: 3411.2 (NH), 3025.9 (CH_{arom}), 1736.6 (C=O), 1617.8 (C=N), 1510.4 (C=C_{arom}); ¹H NMR (600 MHz, DMSO-*d*₆) δ 10.79 (s, 1H), 8.15 (d, *J* = 5.7 Hz, 1H), 7.59 (s, 1H), 6.95 (t, *J* = 9.0 Hz, 1H), 6.67 – 6.61 (m, 1H), 6.49 (dd, *J* = 13.1, 2.2 Hz, 1H), 6.40 (d, *J* = 8.7 Hz, 1H), 5.44 (s, 2H), 2.03 – 1.88 (m, 1H), 0.76 (br, 4H); MS (ESI) *m/z*(%): 288.1 [M+H]⁺, 310.1 [M+Na]⁺.

4.1.4. General procedure for Preparation of the target compounds (**15a-f**, **20a-h** and **26a-i**)

A mixture of the corresponding acids (**14a-f**, **19a-h** or **25a-h**, 1.30 mmol), compound **10** (1.00 mmol), HATU (1.50 mmol), Et₃N (3.00 mmol), and DMF (8 mL) was stirred at room temperature for 12 h. The residue was dissolved in CH₂Cl₂ (50 mL) and the resulting mixture was sequentially washed with 20% K₂CO₃ (30 mL × 3) and brine (30 mL × 3), and the organic phase was separated, dried, and evaporated. The crude product obtained was purified by silica gel chromatography to afford **15a-f**, **20a-h** or **26a-i** as white solids.

4.1.4.1. *N*-(4-((2-(Cyclopropanecarboxamido)pyridin-4-yl)oxy)-3-fluorophenyl)-4-methyl-6-oxo-1-phenyl-1,6-dihydropyridazine-3-carboxamide (**15a**)

Yield: 74.6%; M.p.: 212–215 °C; IR (KBr, cm⁻¹): 3388.9 (NH), 1676.1 (C=O), 1575.8 (C=N), 1500.6 (C=C_{arom}); ¹H NMR (600 MHz, CDCl₃) δ 8.97 (s, 1H), 8.62 (s, 1H), 8.11 (d, *J* = 5.8 Hz, 1H), 7.84 – 7.67 (m, 2H), 7.61 (d, *J* = 7.6 Hz, 2H), 7.54 (t, *J* = 7.8 Hz, 2H), 7.47 (t, *J* = 7.4 Hz, 1H), 7.25 (s, 1H), 7.14 (t, *J* = 8.6 Hz, 1H), 6.91 (d, *J* = 1.0 Hz, 1H), 6.62 (dd, *J* = 5.8, 2.3 Hz, 1H), 2.66 (d, *J* = 0.7 Hz, 3H), 1.51 (m, 1H), 1.03 (dt, *J* = 8.0, 4.0 Hz, 2H), 0.88 – 0.80 (m, 2H); ¹³C NMR (150 MHz, CDCl₃) δ 172.30, 166.08, 160.32, 159.31, 154.23 (d, *J* = 249.7 Hz), 153.21, 148.87, 144.42, 140.51, 137.78, 137.08 (d, *J* = 12.5 Hz), 135.69 (d, *J* = 9.6 Hz), 130.88, 129.03, 128.88, 125.35, 123.51, 116.11, 109.40 (d, *J* = 23.1 Hz), 107.88, 100.54, 20.36, 15.78, 8.29; MS (ESI) *m/z* (%): 500.2 [M+H]⁺.

4.1.4.2. *N*-(4-((2-(Cyclopropanecarboxamido)pyridin-4-yl)oxy)-3-fluorophenyl)-1-(4-fluorophenyl)-4-methyl-6-oxo-1,6-dihydropyridazine-3-carboxamide (**15b**)

Yield: 78.3%; M.p.: 200–202 °C; IR (KBr, cm⁻¹): 3392.8 (NH), 3255.8 (NH), 1674.2 (C=O), 1585.5 (C=N), 1504.5 (C=C_{arom}); ¹H NMR (600 MHz, CDCl₃) δ 8.92 (s, 1H), 8.64 (s, 1H), 8.12 (d, *J* = 5.7 Hz, 1H), 7.82 – 7.68 (m, 2H), 7.60 (dd, *J* = 8.8, 4.7 Hz, 2H), 7.26 – 7.18 (m, 3H), 7.14 (t, *J* = 8.6 Hz, 1H), 6.91 (s, 1H), 6.64 (dd, *J* = 5.7, 2.2 Hz, 1H), 2.66 (s, 3H), 1.57 – 1.45 (m, 1H), 1.11 – 0.97 (m, 2H), 0.93 – 0.79 (m, 2H); ¹³C NMR (150 MHz, CDCl₃) δ 172.33, 166.06, 162.30 (d, *J* = 249.6 Hz), 160.20, 159.24, 154.23 (d, *J* = 249.7 Hz), 153.20, 148.87, 144.57, 137.99, 137.12 (d, *J* = 12.3 Hz), 135.62 (d, *J* = 9.5 Hz), 130.85, 129.63, 128.52, 127.30 (d, *J* = 8.8 Hz), 123.53, 115.97 (d, *J* = 23.1 Hz), 109.43 (d, *J* = 23.2 Hz), 107.97, 100.43, 20.35, 15.78, 8.30; MS (ESI) *m/z* (%): 518.1[M+H]⁺, 540.1[M+Na]⁺, 556.1[M+K].

4.1.4.3. *1-(4-Chlorophenyl)-N-(4-((2-(cyclopropanecarboxamido)pyridin-4-yl)oxy)-3-fluorophenyl)-4-methyl-6-oxo-1,6-dihydropyridazine-3-carboxamide (15c)*

Yield: 81.9%; M.p.: 191–193 °C; IR (KBr, cm⁻¹): 3207.6 (NH), 1664.6 (C=O), 1589.3 (C=N), 1494.8 (C=C_{arom}); ¹H NMR (600 MHz, CDCl₃) δ 8.89 (s, 1H), 8.44 (s, 1H), 8.12 (d, *J* = 5.8 Hz, 1H), 7.82 – 7.66 (m, 2H), 7.59 (d, *J* = 8.8 Hz, 2H), 7.50 (d, *J* = 8.8 Hz, 2H), 7.24 (s, 1H), 7.15 (t, *J* = 8.6 Hz, 1H), 6.92 (t, *J* = 7.4 Hz, 1H), 6.63 (m, 1H), 2.66 (s, 3H), 1.55 – 1.43 (m, 1H), 1.07 – 1.00 (m, 2H), 0.89 – 0.81 (m, 2H); ¹³C NMR (150 MHz, CDCl₃) δ 172.37, 166.05, 160.17, 159.09, 154.21 (d, *J* = 249.6 Hz), 153.26, 148.85, 144.57, 138.87, 138.21, 137.10 (d, *J* = 12.3 Hz), 135.65 (d, *J* = 9.4 Hz), 134.69, 130.85, 129.14, 126.62, 123.50, 116.15, 109.41 (d, *J* = 23.2 Hz), 107.99, 100.44, 20.33, 15.73, 8.29; MS (ESI) *m/z* (%): 534.1 [M+H]⁺, 556.1 [M+Na]⁺.

4.1.4.4. *N-(4-((2-(Cyclopropanecarboxamido)pyridin-4-yl)oxy)-3-fluorophenyl)-1-(2-fluorophenyl)-4-methyl-6-oxo-1,6-dihydropyridazine-3-carboxamide (15d)*

Yield: 74.6%; M.p.: 171–174 °C; IR (KBr, cm⁻¹): 3408.3 (NH), 1670.4 (C=O), 1589.3 (C=N), 1502.6 (C=C_{arom}); ¹H NMR (600 MHz, CDCl₃) δ 8.94 (s, 1H), 8.78 (s, 1H), 8.11 (d, *J* = 5.7 Hz, 1H), 7.74 (d, *J* = 12.1 Hz, 2H), 7.48 (t, *J* = 6.8 Hz, 2H), 7.39 – 7.26 (m, 3H), 7.12 (t, *J* = 8.6 Hz, 1H), 6.92 (s, 1H), 6.67 – 6.57 (m, 1H), 2.66 (s, 3H), 1.56 – 1.45 (m, 1H), 1.07 – 0.97 (m, 2H), 0.91 – 0.78 (m, 2H); MS (ESI) *m/z* (%): 518.1 [M+H]⁺, 540.1 [M+Na]⁺;

4.1.4.5. *1-(2-Chlorophenyl)-N-(4-((2-(cyclopropanecarboxamido)pyridin-4-yl)oxy)-3-fluorophenyl)-4-methyl-6-oxo-1,6-dihydropyridazine-3-carboxamide (15e)*

Yield: 83.7%; M.p.: 173–176 °C; IR (KBr, cm⁻¹): 3402.4 (NH), 3298.9 (NH), 1672.3 (C=O), 1575.8 (C=N), 1517.9 (C=C_{arom}); ¹H NMR (600 MHz, CDCl₃) δ 8.93 (s, 1H), 8.78 (s, 1H), 8.11 (d, *J* = 5.8 Hz, 1H), 7.74 (dd, *J* = 12.0, 2.1 Hz, 2H), 7.63 – 7.54 (m, 1H), 7.52 – 7.40 (m, 3H), 7.25 (s, 1H), 7.12 (t, *J* = 8.7 Hz, 1H), 6.94 (d, *J* = 0.9 Hz, 1H), 6.61 (dd, *J* = 5.8, 2.3 Hz, 1H), 2.68 (s, 3H), 1.56 – 1.43 (m, 1H), 1.06 – 0.98 (m, 2H), 0.87 – 0.80 (m, 2H); MS (ESI) *m/z* (%): 534.1 [M+H]⁺, 556.1 [M+Na]⁺.

4.1.4.6. *N-(4-((2-(Cyclopropanecarboxamido)pyridin-4-yl)oxy)-3-fluorophenyl)-1-(4-methoxyphenyl)-4-methyl-6-oxo-1,6-dihydropyridazine-3-carboxamide (15f)*

Yield: 82.1%; M.p.: 245–247 °C; IR (KBr, cm⁻¹): 3392.8 (NH), 3290.6 (NH), 1656.9 (C=O), 1595.1 (C=N), 1527.6 (C=C_{arom}), 1502.6 (C=C_{arom}); ¹H NMR (600 MHz, CDCl₃) δ 8.98 (s, 1H), 8.55 (s, 1H), 8.11 (d, *J* = 5.8 Hz, 1H), 7.82 – 7.68 (m, 2H), 7.52 (d, *J* = 8.9 Hz, 2H), 7.25 (s, 1H), 7.14 (t, *J* = 8.6 Hz, 1H), 7.03 (d, *J* = 8.9 Hz, 2H), 6.90 (s, 1H), 6.62 (dd, *J* = 5.7, 2.2 Hz, 1H), 3.87 (s, 3H), 2.65 (s, 3H), 1.55 – 1.44 (m, 1H), 1.08 – 1.00 (m, 2H), 0.89 – 0.83 (m, 2H); ¹³C NMR (150 MHz, CDCl₃) δ 172.2, 166.08, 160.38, 159.70, 159.47, 154.24 (d, *J* = 249.7 Hz), 153.19, 148.89, 144.27, 137.52, 137.05 (d, *J* = 12.6 Hz), 135.73 (d, *J* = 9.4 Hz), 133.48, 130.70, 126.58, 123.50, 116.08, 114.16, 109.37 (d, *J* = 22.9 Hz), 107.88, 100.53, 55.54, 20.34, 15.79, 8.28; MS (ESI) *m/z* (%): 530.2 [M+H]⁺.

4.1.4.7. *N-(4-((2-(Cyclopropanecarboxamido)pyridin-4-yl)oxy)-3-fluorophenyl)-5-methyl-4-oxo-1-phenyl-1,4-dihydropyridazine-3-carboxamide (20a)*

Yield: 74.7%; M.p.: 262–265 °C; IR (KBr, cm⁻¹): 3248.1 (NH), 3047.5 (CH_{arom}), 1685.8 (C=O), 1543.1 (C=N); ¹H NMR (600 MHz, DMSO-*d*₆) δ 12.30 (s, 1H), 10.88 (s, 1H), 9.11 (d, *J* = 0.6 Hz, 1H), 8.21 (d, *J* = 5.7 Hz, 1H), 7.99 (dd, *J* = 12.7, 2.3 Hz, 1H), 7.84 (d, *J* = 7.7 Hz, 2H), 7.71 – 7.60 (m, 3H), 7.53 (t, *J* = 7.4 Hz, 2H), 7.40 (t, *J* = 8.9 Hz, 1H), 6.74 (dd, *J* = 5.7, 2.4 Hz, 1H), 2.14 (s, 3H), 2.01 – 1.93 (m, 1H), 0.81 – 0.73 (m, 4H); ¹³C NMR (150 MHz, CDCl₃) δ 172.14, 171.18, 166.22, 159.47, 154.20 (d, *J* = 248.3 Hz), 153.08, 148.90, 143.34, 142.24, 138.21, 136.97 (d, *J* = 12.7 Hz), 136.76 (d, *J* = 9.6 Hz), 133.17, 129.91, 129.63, 129.19, 128.52, 123.38, 121.62, 116.56, 109.83 (d, *J* = 23.6 Hz), 107.58, 100.95, 15.84, 13.61, 8.27; MS (ESI) *m/z* (%): 500.1 [M+H]⁺, 522.1 [M+Na]⁺.

4.1.4.8. *N-(4-((2-(Cyclopropanecarboxamido)pyridin-4-yl)oxy)-3-fluorophenyl)-1-(4-fluorophenyl)-5-methyl-4-oxo-1,4-dihydropyridazine-3-carboxamide (20b)*

Yield: 68.3%; M.p.: 179–181 °C; IR (KBr, cm⁻¹): 3423.7 (NH), 1683.9 (C=O), 1545.0 (C=N), 1496.8 (C=C_{arom});

^1H NMR (600 MHz, DMSO- d_6) δ 12.22 (s, 1H), 10.81 (s, 1H), 9.00 (s, 1H), 8.14 (d, J = 5.7 Hz, 1H), 7.92 (dd, J = 12.7, 2.3 Hz, 1H), 7.86 – 7.77 (m, 2H), 7.59 (d, J = 2.1 Hz, 1H), 7.44 (dd, J = 14.4, 5.0 Hz, 3H), 7.33 (t, J = 8.9 Hz, 1H), 6.67 (dd, J = 5.7, 2.4 Hz, 1H), 2.48 – 2.40 (m, 3H), 1.95 – 1.84 (m, 1H), 0.74 – 0.65 (m, 4H); ^{13}C NMR (150 MHz, DMSO- d_6) δ 173.27, 170.02, 165.70, 162.01 (d, J = 246.0 Hz), 160.51, 154.32, 153.89 (d, J = 246.2 Hz), 149.98, 144.21, 140.23, 139.97 (d, J = 2.7 Hz), 137.42 (d, J = 9.9 Hz), 136.26 (d, J = 12.3 Hz), 131.78, 124.62, 124.28 (d, J = 9.0 Hz), 116.97, 116.82, 108.93 (d, J = 22.9 Hz), 107.57, 99.65, 14.59, 13.31, 8.09; MS (ESI) m/z (%): 518.2 $[\text{M}+\text{H}]^+$, 540.1 $[\text{M}+\text{Na}]^+$.

4.1.4.9. *1-(4-Chlorophenyl)-N-(4-((2-(cyclopropanecarboxamido)pyridin-4-yl)oxy)-3-fluorophenyl)-5-methyl-4-oxo-1,4-dihydropyridazine-3-carboxamide*. (**20c**).

Yield: 84.0%; M.p.: 204-207 °C; IR (KBr, cm^{-1}): 3417.9 (NH), 1672.3 (C=O), 1550.8 (C=N), 1492.9 (C=C_{arom}); ^1H NMR (600 MHz, DMSO- d_6) δ 12.21 (s, 1H), 10.88 (s, 1H), 9.11 (s, 1H), 8.21 (d, J = 5.7 Hz, 1H), 7.98 (dd, J = 12.7, 2.2 Hz, 1H), 7.88 (d, J = 8.9 Hz, 2H), 7.70 (d, J = 8.9 Hz, 2H), 7.66 (d, J = 2.1 Hz, 1H), 7.56 – 7.49 (m, 1H), 7.40 (t, J = 8.9 Hz, 1H), 6.74 (dd, J = 5.7, 2.4 Hz, 1H), 2.13 (s, 3H), 2.01 – 1.94 (m, 1H), 0.81 – 0.73 (m, 4H); ^{13}C NMR (150 MHz, CDCl_3) δ 172.28, 171.16, 166.19, 159.26, 154.18 (d, J = 248.9 Hz), 153.24, 148.86, 142.20, 141.66, 137.76, 137.00 (d, J = 12.3 Hz), 136.65 (d, J = 9.4 Hz), 135.18, 133.30, 130.02, 123.40, 122.69, 116.53, 109.79 (d, J = 22.9 Hz), 107.64, 100.92, 15.76, 13.58, 8.27; MS (ESI) m/z (%): 534.1 $[\text{M}+\text{H}]^+$, 556.1 $[\text{M}+\text{Na}]^+$.

4.1.4.10. *N-(4-((2-(Cyclopropanecarboxamido)pyridin-4-yl)oxy)-3-fluorophenyl)-1-(2-fluorophenyl)-5-methyl-4-oxo-1,4-dihydropyridazine-3-carboxamide*. (**20d**).

Yield: 75.4%; M.p.: 178-180 °C; IR (KBr, cm^{-1}): 3477.7 (NH), 3261.6 (NH), 3030.2 (CH_{arom}), 1687.7 (C=O), 1496.8 (C=C_{arom}), 1417.7; ^1H NMR (600 MHz, CDCl_3) δ 12.66 (s, 1H), 8.57 (s, 1H), 8.22 (d, J = 1.0 Hz, 1H), 8.11 (d, J = 5.8 Hz, 1H), 7.99 (dd, J = 12.2, 2.3 Hz, 1H), 7.81 (s, 1H), 7.74 (td, J = 7.9, 1.3 Hz, 1H), 7.48 (dd, J = 21.2, 14.4 Hz, 2H), 7.39 – 7.28 (m, 2H), 7.16 (t, J = 8.7 Hz, 1H), 6.59 (dd, J = 5.8, 2.3 Hz, 1H), 2.26 (s, 3H), 1.57 – 1.47 (m, 1H), 1.10 – 1.03 (m, 2H), 0.89 – 0.82 (m, 2H); MS (ESI) m/z (%): 518.1 $[\text{M}+\text{H}]^+$, 540.1 $[\text{M}+\text{Na}]^+$.

4.1.4.11. *N-(4-((2-(Cyclopropanecarboxamido)pyridin-4-yl)oxy)-3-fluorophenyl)-1-(4-methoxyphenyl)-5-methyl-4-oxo-1,4-dihydropyridazine-3-carboxamide* (**20e**).

Yield: 76.6%; M.p.: 173-176 °C; IR (KBr, cm^{-1}): 3420.6 (NH), 3010.8 (CH_{arom}), 1687.7 (C=O), 1504.5 (C=C_{arom}); ^1H NMR (600 MHz, DMSO- d_6) δ 12.44 (s, 1H), 10.88 (s, 1H), 9.03 (s, 1H), 8.22 (d, J = 5.6 Hz, 1H), 8.00 (d, J = 12.6 Hz, 1H), 7.76 (d, J = 8.9 Hz, 2H), 7.67 (s, 1H), 7.53 (d, J = 8.6 Hz, 1H), 7.40 (t, J = 8.8 Hz, 1H), 7.17 (d, J = 8.9 Hz, 2H), 6.75 (d, J = 3.5 Hz, 1H), 3.85 (s, 3H), 2.14 (s, 3H), 2.03 – 1.92 (m, 1H), 0.84 – 0.68 (m, 4H); ^{13}C NMR (150 MHz, DMSO- d_6) δ 173.27, 169.96, 165.71, 160.55, 159.68, 154.32, 153.90 (d, J = 246.2 Hz), 149.97, 143.62, 140.18, 137.46 (d, J = 9.7 Hz), 136.92, 136.23 (d, J = 12.3 Hz), 132.06, 124.60, 123.40, 116.95, 115.06, 108.93 (d, J = 22.9 Hz), 107.56, 99.67, 56.04, 14.59, 13.32, 8.09; MS (ESI) m/z (%): 530.2 $[\text{M}+\text{H}]^+$, 552.1 $[\text{M}+\text{Na}]^+$.

4.1.4.12. *N-(4-((2-(Cyclopropanecarboxamido)pyridin-4-yl)oxy)-3-fluorophenyl)-5-methyl-4-oxo-1-(4-(trifluoromethyl)phenyl)-1,4-dihydropyridazine-3-carboxamide* (**20f**).

Yield: 69.2%; M.p.: 172-174 °C; IR (KBr, cm^{-1}): 3238.5 (NH), 1687.7 (C=O), 1560.4 (C=N), 1510.3 (C=C_{arom}), 1321.2 (CF₃); ^1H NMR (600 MHz, DMSO- d_6) δ 12.07 (s, 1H), 10.88 (s, 1H), 9.20 (d, J = 0.7 Hz, 1H), 8.21 (d, J = 5.7 Hz, 1H), 8.10 (d, J = 8.6 Hz, 2H), 8.05 – 7.95 (m, 3H), 7.65 (d, J = 2.3 Hz, 1H), 7.54 (dd, J = 8.9, 1.4 Hz, 1H), 7.41 (t, J = 8.9 Hz, 1H), 6.75 (dd, J = 5.7, 2.4 Hz, 1H), 2.14 (s, 3H), 2.01 – 1.93 (m, 1H), 0.77 (t, J = 5.6 Hz, 4H); MS (ESI) m/z (%): 568.2 $[\text{M}+\text{H}]^+$, 590.1 $[\text{M}+\text{Na}]^+$.

4.1.4.13. *1-(3-Chloro-4-fluorophenyl)-N-(4-((2-(cyclopropanecarboxamido)pyridin-4-yl)oxy)-3-fluorophenyl)-5-methyl-4-oxo-1,4-dihydropyridazine-3-carboxamide* (**20g**).

Yield: 81.5%; M.p.: 194-197 °C; IR (KBr, cm^{-1}): 3427.5 (NH), 1695.4 (C=O), 1552.7 (C=N), 1500.6 (C=C_{arom}); ^1H NMR (600 MHz, DMSO- d_6) δ 12.17 (s, 1H), 10.88 (s, 1H), 9.11 (s, 1H), 8.26 – 8.11 (m, 2H), 8.05 – 7.94 (m, 1H), 7.92 – 7.84 (m, 1H), 7.68 (dd, J = 28.8, 5.5 Hz, 2H), 7.54 (d, J = 8.6 Hz, 1H), 7.40 (t, J = 8.9 Hz, 1H), 6.74 (dd, J =

5.7, 2.3 Hz, 1H), 2.12 (s, 3H), 2.02 – 1.92 (m, 1H), 0.82 – 0.73 (m, 4H); MS (ESI) m/z (%): 552.1 $[M+H]^+$, 574.1 $[M+Na]^+$.

4.1.4.14. *N*-(4-((2-(Cyclopropanecarboxamido)pyridin-4-yl)oxy)-3-fluorophenyl)-1-(3,4-dimethoxyphenyl)-5-methyl-4-oxo-1,4-dihydropyridazine-3-carboxamide (**20h**).

Yield: 86.1%; M.p.: 288-290 °C; IR (KBr, cm^{-1}): 3248.1 (NH), 1687.7 (C=O), 1563.2 (C=N), 1502.6 (C=C_{arom}); ¹H NMR (600 MHz, DMSO-*d*₆) δ 12.42 (s, 1H), 10.88 (s, 1H), 9.03 (s, 1H), 8.21 (d, $J = 5.7$ Hz, 1H), 8.00 (dd, $J = 12.7, 2.3$ Hz, 1H), 7.66 (d, $J = 2.2$ Hz, 1H), 7.52 (dd, $J = 8.8, 1.3$ Hz, 1H), 7.43 – 7.31 (m, 3H), 7.16 (d, $J = 8.8$ Hz, 1H), 6.74 (dd, $J = 5.7, 2.4$ Hz, 1H), 3.87 (s, 3H), 3.84 (s, 3H), 2.14 (s, 3H), 2.02 – 1.93 (m, 1H), 0.81 – 0.73 (m, 4H); ¹³C NMR (150 MHz, DMSO-*d*₆) δ 173.27, 169.96, 165.71, 160.54, 154.32, 153.90 (d, $J = 246.2$ Hz), 149.97, 149.47, 149.38, 143.59, 140.28, 137.46 (d, $J = 9.7$ Hz), 136.90, 136.23 (d, $J = 12.3$ Hz), 131.97, 124.59, 116.95, 114.21, 112.14, 108.93 (d, $J = 22.9$ Hz), 107.57, 106.26, 99.66, 56.34, 56.25, 14.59, 13.32, 8.09; MS (ESI) m/z (%): 560.2 $[M+H]^+$, 582.2 $[M+Na]^+$.

4.1.4.15. *N*-(4-((2-(Cyclopropanecarboxamido)pyridin-4-yl)oxy)-3-fluorophenyl)-4-methyl-3,5-dioxo-2-phenyl-2,3,4,5-tetrahydro-1,2,4-triazine-6-carboxamide (**26a**).

Yield: 76.4%; M.p.: 247-249 °C; IR (KBr, cm^{-1}): 3416.7 (NH), 3246.5 (NH), 3060.4 (CH_{arom}), 2851.6 (CH_{aryl}), 1738.7 (C=O), 1698.5 (C=O), 1660.6 (C=O), 1578.5 (C=N), 1507.5 (C=C_{arom}); ¹H NMR (600 MHz, DMSO-*d*₆) δ 10.96 (s, 1H), 10.88 (s, 1H), 8.22 (d, $J = 5.6$ Hz, 1H), 7.90 (d, $J = 12.5$ Hz, 1H), 7.66 (s, 1H), 7.63 – 7.52 (m, 5H), 7.48 (t, $J = 7.1$ Hz, 1H), 7.41 (t, $J = 8.9$ Hz, 1H), 6.74 (d, $J = 5.5$ Hz, 1H), 3.31 (s, 3H), 2.06 – 1.92 (m, 1H), 0.89 – 0.67 (m, 4H); ¹³C NMR (150 MHz, DMSO-*d*₆) δ 173.27, 165.65, 158.91, 155.06, 154.33, 153.80 (d, $J = 246.1$ Hz), 149.98, 148.47, 140.46, 137.09 (d, $J = 9.7$ Hz), 136.51, 136.45, 129.25, 128.93, 126.20, 124.57, 117.14, 109.08 (d, $J = 22.9$ Hz), 107.57, 99.66, 27.76, 14.60, 8.09; MS (ESI) m/z (%): 517.2 $[M+H]^+$.

4.1.4.16. *N*-(4-((2-(Cyclopropanecarboxamido)pyridin-4-yl)oxy)-3-fluorophenyl)-2-(4-fluorophenyl)-4-methyl-3,5-dioxo-2,3,4,5-tetrahydro-1,2,4-triazine-6-carboxamide (**26b**).

Yield: 82.4%; M.p.: 265-268 °C; IR (KBr, cm^{-1}): 3416.9 (NH), 3236.3 (NH), 2934.0 (CH_{aryl}), 1725.7 (C=O), 1695.2 (C=O), 1610.3 (C=N), 1552.8 (C=N), 1508.0 (C=C_{arom}); ¹H NMR (600 MHz, DMSO-*d*₆) δ 10.93 (s, 1H), 10.88 (s, 1H), 8.21 (d, $J = 5.7$ Hz, 1H), 7.89 (dd, $J = 12.6, 2.3$ Hz, 1H), 7.70 – 7.60 (m, 3H), 7.55 (dd, $J = 8.8, 1.3$ Hz, 1H), 7.45 – 7.34 (m, 3H), 6.74 (dd, $J = 5.7, 2.4$ Hz, 1H), 3.30 (s, 3H), 2.03 – 1.90 (m, 1H), 0.77 (t, $J = 5.9$ Hz, 4H); ¹³C NMR (150 MHz, DMSO-*d*₆) δ 173.28, 165.65, 161.84 (d, $J = 246.0$ Hz), 158.85, 155.01, 154.32, 153.79 (d, $J = 246.5$ Hz), 149.98, 148.53, 137.07 (d, $J = 9.9$ Hz), 136.76 (d, $J = 2.9$ Hz), 136.52, 128.58, 128.52, 124.57, 117.14, 116.22, 116.07, 109.10 (d, $J = 23.1$ Hz), 107.59, 99.63, 27.76, 14.59, 8.09; MS (ESI) m/z (%): 535.2 $[M+H]^+$, 557.1 $[M+Na]^+$.

4.1.4.17. 2-(4-Chlorophenyl)-*N*-(4-((2-(cyclopropanecarboxamido)pyridin-4-yl)oxy)-3-fluorophenyl)-4-methyl-3,5-dioxo-2,3,4,5-tetrahydro-1,2,4-triazine-6-carboxamide (**26c**).

Yield: 85.3%; M.p.: 284-286 °C; IR (KBr, cm^{-1}): 3414.1 (NH), 3250.2 (NH), 3076.9 (CH_{arom}), 2923.1 (CH_{aryl}), 1734.6 (C=O), 1691.1 (C=O), 1665.3 (C=O), 1579.4 (C=N), 1504.9 (C=C_{arom}); ¹H NMR (600 MHz, CDCl₃) δ 10.92 (s, 1H), 8.45 (s, 1H), 8.12 (d, $J = 5.7$ Hz, 1H), 7.88 (dd, $J = 11.9, 2.2$ Hz, 1H), 7.77 (s, 1H), 7.57 (d, $J = 8.8$ Hz, 2H), 7.48 (d, $J = 8.8$ Hz, 2H), 7.38 (d, $J = 8.1$ Hz, 1H), 7.19 (t, $J = 8.6$ Hz, 1H), 6.63 (dd, $J = 5.7, 2.2$ Hz, 1H), 3.54 (s, 3H), 1.55 – 1.45 (m, 1H), 1.12 – 0.97 (m, 2H), 0.91 – 0.76 (m, 2H); ¹³C NMR (150 MHz, CDCl₃) δ 172.37, 166.05, 156.43, 156.16, 154.19 (d, $J = 249.8$ Hz), 153.26, 148.83, 147.35, 138.02, 137.53 (d, $J = 12.4$ Hz), 135.71 (d, $J = 9.4$ Hz), 134.97, 132.40, 129.25, 126.35, 123.56, 116.55, 109.90 (d, $J = 23.3$ Hz), 107.83, 100.75, 28.21, 15.75, 8.30; MS (ESI) m/z (%): 551.1 $[M+H]^+$, 573.2 $[M+Na]^+$.

4.1.4.18. *N*-(4-((2-(Cyclopropanecarboxamido)pyridin-4-yl)oxy)-3-fluorophenyl)-2-(2-fluorophenyl)-4-methyl-3,5-dioxo-2,3,4,5-tetrahydro-1,2,4-triazine-6-carboxamide (**26d**).

Yield: 71.9%; M.p.: 249-252 °C; IR (KBr, cm^{-1}): 3336.9 (NH), 1737.9 (C=O), 1697.4 (C=O), 1595.1 (C=N),

1498.7 (C=C_{arom}); ¹H NMR (600 MHz, DMSO-*d*₆) δ 10.98 (s, 1H), 10.87 (s, 1H), 8.20 (d, *J* = 5.7 Hz, 1H), 7.87 (dd, *J* = 12.6, 2.2 Hz, 1H), 7.68 – 7.34 (m, 7H), 6.73 (dd, *J* = 5.7, 2.4 Hz, 1H), 3.30 (s, 3H), 1.96 (m, 1H), 0.77 (t, *J* = 6.3 Hz, 4H); MS (ESI) *m/z* (%): 535.1 [M+H]⁺, 557.1 [M+Na]⁺.

4.1.4.19. *N*-(4-((2-(Cyclopropanecarboxamido)pyridin-4-yl)oxy)-3-fluorophenyl)-2-(4-methoxyphenyl)-4-methyl-3,5-dioxo-2,3,4,5-tetrahydro-1,2,4-triazine-6-carboxamide (**26e**).

Yield: 83.7%; M.p.: 210-212 °C; IR (KBr, cm⁻¹): 3415.5 (NH), 3238.4 (NH), 3065.9 (CH_{arom}), 2917.6 (CH_{aryl}), 1736.4 (C=O), 1697.7 (C=O), 1663.0 (C=O), 1608.6 (C=N), 1578.3 (C=N), 1541.8 (C=C_{arom}), 1511.8 (C=C_{arom}); ¹H NMR (600 MHz, DMSO-*d*₆) δ 10.93 (s, 1H), 10.88 (s, 1H), 8.21 (d, *J* = 5.7 Hz, 1H), 7.90 (dd, *J* = 12.6, 2.2 Hz, 1H), 7.65 (d, *J* = 2.2 Hz, 1H), 7.59 – 7.52 (m, 1H), 7.49 (d, *J* = 8.9 Hz, 2H), 7.40 (t, *J* = 8.9 Hz, 1H), 7.08 (d, *J* = 9.0 Hz, 2H), 6.73 (dd, *J* = 5.7, 2.4 Hz, 1H), 3.82 (s, 3H), 3.30 (s, 3H), 2.03 – 1.91 (m, 1H), 0.77 (t, *J* = 6.7 Hz, 4H); ¹³C NMR (150 MHz, DMSO-*d*₆) δ 173.27, 165.65, 159.46, 158.93, 155.16, 154.33, 153.80 (d, *J* = 246.1 Hz), 149.98, 148.60, 137.10 (d, *J* = 9.9 Hz), 136.47 (d, *J* = 12.2 Hz), 136.08, 133.42, 127.62, 124.56, 117.12, 114.35, 109.06 (d, *J* = 23.0 Hz), 107.57, 99.66, 55.88, 27.77, 14.59, 8.09; MS (ESI) *m/z* (%): 547.2 [M+H]⁺.

4.1.4.20. *N*-(4-((2-(Cyclopropanecarboxamido)pyridin-4-yl)oxy)-3-fluorophenyl)-2-(3-fluorophenyl)-4-methyl-3,5-dioxo-2,3,4,5-tetrahydro-1,2,4-triazine-6-carboxamide (**26f**).

Yield: 74.1%; M.p.: 255-257 °C; IR (KBr, cm⁻¹): 3416.9 (NH), 3243.6 (NH), 3065.9 (CH_{arom}), 2934.1 (CH_{aryl}), 1740.7 (C=O), 1700.8 (C=O), 1662.9 (C=O), 1601.0 (C=N), 1547.6 (C=C_{arom}); ¹H NMR (600 MHz, DMSO-*d*₆) δ 10.92 (s, 1H), 10.88 (s, 1H), 8.21 (d, *J* = 5.6 Hz, 1H), 7.90 (d, *J* = 12.5 Hz, 1H), 7.72 – 7.29 (m, 7H), 6.81 – 6.64 (m, 1H), 3.31 (s, 3H), 1.97 (d, *J* = 4.9 Hz, 1H), 0.86 – 0.70 (m, 4H); ¹³C NMR (150 MHz, DMSO-*d*₆) δ 173.28, 165.65, 161.97 (d, *J* = 244.3 Hz), 158.80, 154.78, 154.33, 153.79 (d, *J* = 246.1 Hz), 149.98, 148.33, 141.64 (d, *J* = 10.5 Hz), 137.06 (d, *J* = 9.6 Hz), 136.84, 136.52 (d, *J* = 12.2 Hz), 130.95 (d, *J* = 9.0 Hz), 124.56, 122.28, 117.20, 115.82 (d, *J* = 20.8 Hz), 113.50 (d, *J* = 25.0 Hz), 109.14 (d, *J* = 23.1 Hz), 107.58, 99.65, 27.77, 14.59, 8.09; MS (ESI) *m/z* (%): 535.2 [M+H]⁺.

4.1.4.21. 2-(3-Chlorophenyl)-*N*-(4-((2-(cyclopropanecarboxamido)pyridin-4-yl)oxy)-3-fluorophenyl)-4-methyl-3,5-dioxo-2,3,4,5-tetrahydro-1,2,4-triazine-6-carboxamide (**26g**).

Yield: 81.4%; M.p.: 175-178 °C; IR (KBr, cm⁻¹): 3415.8 (NH), 3263.7 (NH), 3071.4 (CH_{arom}), 2851.6 (CH_{aryl}), 1735.1 (C=O), 1688.6 (C=O), 1661.0 (C=O), 1578.9 (C=N), 1548.1 (C=C_{arom}), 1506.1 (C=C_{arom}); ¹H NMR (600 MHz, CDCl₃) δ 10.90 (s, 1H), 8.76 (s, 1H), 8.12 (d, *J* = 5.7 Hz, 1H), 7.88 (d, *J* = 11.8 Hz, 1H), 7.78 (s, 1H), 7.64 (s, 1H), 7.52 (d, *J* = 3.5 Hz, 1H), 7.47 – 7.34 (m, 3H), 7.18 (t, *J* = 8.6 Hz, 1H), 6.71 – 6.55 (m, 1H), 3.53 (s, 3H), 1.59 – 1.47 (m, 1H), 1.10 – 1.00 (m, 2H), 0.90 – 0.79 (m, 2H); MS (ESI) *m/z* (%): 551.1 [M+H]⁺, 573.1 [M+Na]⁺.

4.1.4.22. 2-(3-Chloro-4-fluorophenyl)-*N*-(4-((2-(cyclopropanecarboxamido)pyridin-4-yl)oxy)-3-fluorophenyl)-4-methyl-3,5-dioxo-2,3,4,5-tetrahydro-1,2,4-triazine-6-carboxamide (**26h**).

Yield: 79.4%; M.p.: 174-176 °C; IR (KBr, cm⁻¹): 3420.5 (NH), 3257.8 (NH), 3070.9 (CH_{arom}), 2923.1 (CH_{aryl}), 1741.8 (C=O), 1660.3 (C=O), 1600.9 (C=N), 1578.4 (C=N), 1547.2 (C=C_{arom}), 1499.2 (C=C_{arom}); ¹H NMR (600 MHz, DMSO-*d*₆) δ 10.91 (s, 1H), 10.88 (s, 1H), 8.21 (d, *J* = 5.7 Hz, 1H), 7.97 – 7.80 (m, 2H), 7.63 (dt, *J* = 17.8, 6.6 Hz, 3H), 7.55 (d, *J* = 8.7 Hz, 1H), 7.40 (t, *J* = 8.9 Hz, 1H), 6.74 (dd, *J* = 5.7, 2.3 Hz, 1H), 3.30 (s, 3H), 2.02 – 1.91 (m, 1H), 0.81 – 0.71 (m, 4H); MS (ESI) *m/z* (%): 569.1 [M+H]⁺, 591.1 [M+Na]⁺.

4.1.4.23. *N*-(4-((2-(Cyclopropanecarboxamido)pyridin-4-yl)oxy)-3-fluorophenyl)-2-(3,4-dimethoxyphenyl)-4-methyl-3,5-dioxo-2,3,4,5-tetrahydro-1,2,4-triazine-6-carboxamide (**26i**).

Yield: 82.2%; M.p.: 208-211 °C; IR (KBr, cm⁻¹): 3415.0 (NH), 3252.7 (NH), 2923.1 (CH_{aryl}), 2846.2 (CH_{aryl}), 1722.9 (C=O), 1702.2 (C=O), 1604.0 (C=N), 1550.1 (C=C_{arom}), 1508.5 (C=C_{arom}); ¹H NMR (600 MHz, CDCl₃) δ 10.96 (s, 1H), 8.57 (s, 1H), 8.12 (d, *J* = 5.8 Hz, 1H), 7.89 (dd, *J* = 11.9, 2.2 Hz, 1H), 7.78 (d, *J* = 1.5 Hz, 1H), 7.39 (d, *J* = 8.8 Hz, 1H), 7.21 – 7.11 (m, 2H), 7.07 (d, *J* = 2.4 Hz, 1H), 6.94 (d, *J* = 8.7 Hz, 1H), 6.63 (dd, *J* = 5.8, 2.3 Hz, 1H), 3.93 (s, 3H), 3.91 (s, 3H), 3.54 (s, 3H), 1.57 – 1.50 (m, 1H), 1.09 – 1.03 (m, 2H), 0.89 – 0.83 (m, 2H); ¹³C

NMR (150 MHz, CDCl_3) δ 172.34, 166.12, 156.57, 156.43, 154.19 (d, $J = 249.7$ Hz), 153.20, 149.64, 149.08, 148.73, 147.70, 137.42 (d, $J = 12.6$ Hz), 135.84 (d, $J = 9.2$ Hz), 132.59, 131.79, 123.53, 117.96, 116.50, 110.75, 109.87 (d, $J = 23.2$ Hz), 108.93, 107.81, 100.75, 56.09, 28.18, 15.76, 8.32; MS (ESI) m/z (%): 577.2[M+H]⁺, 599.2[M+Na]⁺.

4.2. Pharmacology

4.2.1. *c-Met* kinase assay

The *in vitro* kinase assays were performed by mobility shift assay. The solution of peptide substrates, ATP, appropriate kinase (Carna), and various concentrations of tested compounds were mixed with the kinase reaction buffer (50 mM HEPES, pH 7.5, 0.0015% Brij-35, 10 mM MgCl_2 , 2 mM DTT), with blank DMSO as the negative control. The kinase reaction was initiated by the addition of tyrosine kinase proteins diluted in 39 μL of kinase reaction buffer solution and incubated at 28 °C for 1 h. Then, 25 μL of stop buffer (100 mM HEPES, pH = 7.5, 0.015% Brij-35, 0.2% Coating Reagent #3, 50 mM EDTA) was added to stop reaction. The data were collected on Caliper at 320 nm and 615 nm and converted to inhibition values. IC_{50} was presented in MS Excel and the curves fitted by XLfit excel add-in version

4.2.2. MTT assay *in vitro*

The anti-proliferative activities of compounds **15a-f**, **20a-h** or **26a-h** were evaluated against A549, H460 and HT-29 cell lines using the standard MTT assay *in vitro*, with Foretinib as the positive control. The cancer cell lines were cultured in minimum essential medium (MEM) supplement with 10% fetal bovine serum (FBS). Approximate 4×10^3 cells, suspended in MEM medium, were plated onto each well of a 96-well plate and incubated in 5% CO_2 at 37 °C for 24 h. The tested compounds at the indicated final concentrations were added to the culture medium and the cell cultures were continued for 72 h. Fresh MTT was added to each well at a terminal concentration of 5 $\mu\text{g}/\text{mL}$, and incubated with cells at 37 °C for 4 h. The formazan crystals were dissolved in 100 μL DMSO each well, and the absorbency at 492 nm (for absorbance of MTT formazan) and 630 nm (for the reference wavelength) was measured with an ELISA reader. All compounds were tested three times in each of the cell lines. The results expressed as IC_{50} (inhibitory concentration 50%) were the averages of three determinations and calculated by using the Bacus Laboratories Incorporated Slide Scanner (Bliss) software.

4.2.3. Soft agar colony-formation assay

The colony formation assay has been the gold standard for determining the effects of cytotoxic agents on cancer cell growth *in vitro* [32]. Briefly, HT-29 cells (1×10^5) in 300 μL RPMI1640 15% FBS medium were diluted in 300 μL of 0.4% agar containing various concentrations of **26a** to give a final agar concentration of 0.2%. The cells-agar mixture was poured over a hardened agar base in wells of 24-well plates and allowed to solidify. Once the top layer solidified, 500 μL of RPMI 1640 medium containing 15% FBS was placed on top to keep the agar moist. Cells were grown at 37 °C in a 5% CO_2 humidified atmosphere for 7 days. Then 100 μL of MTT solution was added to each well, and after 4 hours of incubation at 37 °C, photographs were captured

4.2.4. AO/EB assay

HT-29 cells were added to a final concentration of $1 \times 10^6/\text{mL}$ in a 6-well plate, and the plate was incubated for 24 h. Cells were treated with various concentrations of compound **26a**. After being cultured for 48 h, control cells and treated cells were washed with PBS which stored at 4 °C, and then dual fluorescent staining solution (20 μL) containing 100 $\mu\text{g}/\text{mL}$ AO and 100 $\mu\text{g}/\text{mL}$ EB was added to each well for 10 min, and then covered with a coverslip. The morphology of apoptotic cells was examined using fluorescent microscope.

4.2.5. Apoptosis assay

Apoptosis was measured by flow cytometry using Annexin V/propidium iodide (PI) double staining. HT-29 or A549 cells were added to a final concentration of 1×10^6 /mL in a 6-well plate, and the plate was incubated for 24 h. Cells were treated with various concentrations of compound **26a**. After being cultured for 48 h, control cells and treated cells were harvested and washed with PBS, and then resuspended in 100 μ L 1 \times binding buffer incubated in the mixture of 5 μ L Annexin V-FTIC and 5 μ L PI for 10 min at room temperature in dark place. The cells were resuspended in 400 μ L 1 \times binding buffer just before flow cytometric analysis.

4.2.6. Wound-healing assay

A549 cells were added to a final concentration of 1×10^6 /mL in a 6-well plate, and the plate was incubated for 24 h. Twenty-four hours later, when the cells reached confluency, scratches were created with sterile 1.0 mL pipette tips and images were captured using phase contrast microscopy at 0 h, 12 h, 36 h and 72 h after treatment with 1.0 μ M of compound **26a**.

Acknowledgments

The authors thank the financial support of Shenyang Science & Technology project (project no. 18-013-0-03), National Natural Science Foundation of China (project no. 21807055), Natural Science Foundation of Liaoning Provincial Department of science and technology (project no. 2019-ZD-0191), and Pre-declaration Foundation of Liaoning University (project no. LDGY2019002).

Appendix A. Supplementary data

Supplementary data associated with this article can be found in the online version,

References and notes

- [1] D.P. Bottaro, J.S. Rubin, D.L. Faletto, A.M. Chan, T.E. Kmiecik, G.F. Vande Woude, S.A. Aaronson, Identification of the hepatocyte growth factor receptor as the c-met proto-oncogene product, *Science*. 251 (1991) 802-804.
- [2] M. Jeffers, S. Rong, G.F. Vande Woude, Enhanced tumorigenicity and invasion-metastasis by hepatocyte growth factor/scatter factor-met signalling in human cells concomitant with induction of the urokinase proteolysis network, *Mol. Cell. Biol.* 16 (1996) 1115-1125.
- [3] K. Matsumoto, K. Date, H. Shimura, T. Nakamura, Acquisition of invasive phenotype in gallbladder cancer cells via mutual interaction of stromal fibroblasts and cancer cells as mediated by hepatocyte growth factor, *Jpn. J. Cancer Res.* 87 (1996) 702-710.
- [4] P.M. Comoglio, S. Giordano, L. Trusolino, Drug development of MET inhibitors: targeting oncogene addiction and expedience, *Nat Rev. Drug. Discov.* 7 (2008) 504-516.
- [5] P.K. Parikh, M.D. Ghate, Recent advances in the discovery of small molecule c-Met Kinase inhibitors. *Eur. J. Med Chem.* 143(2018) 1103-1138.
- [6] S. Berthou, D.M. Aebbersold, L.S. Schmidt, D. Stroka, C. Heigl, B. Streit, D. Stalder, G. Gruber, C. Liang, A.R. Howlett, D. Candinas, R.H. Greiner, K.E. Lipson, Y. Zimmer, The Met kinase inhibitor SU11274 exhibits a selective inhibition pattern toward different receptor mutated variants, *Oncogene*. 23 (2004) 5387-5393.
- [7] S.G. Buchanan, J. Hendle, P.S. Lee, C.R. Smith, P.Y. Bounaud, K.A. Jessen, C.M. Tang, N.H. Huser, J.D. Felce, K.J. Froning, M.C. Peterman, B.E. Aubol, S.F. Gessert, J.M. Sauder, K.D. Schwinn, M. Russell, I.A. Rooney, J. Adams, B.C. Leon, T.H. Do, J.M. Blaney, P.A. Sprengeler, D.A. Thompson, L. Smyth, L.A. Pelletier, S. Atwell, K. Holme, S.R. Wasserman, S. Emtage, S.K. Burley, S.H. Reich, SGX523 is an exquisitely selective, ATP-competitive inhibitor of the MET receptor tyrosine kinase with antitumor activity in vivo, *Mol. Cancer Ther.* 8 (2009) 3181-3190.
- [8] M.H. Norman, L. Liu, M. Lee, N. Xi, I. Fellows, N.D. D'Angelo, C. Dominguez, K. Rex, S.F. Bellon, T. S. Kim, I. Dussault, Structure-based design of novel class II c-Met inhibitors: 1. Identification of pyrazolone-based derivatives, *J. Med. Chem.* 55(2012)

1858-1867.

- [9] F.M. Yakes, J. Chen, J. Tan, K. Yamaguchi, Y. Shi, P. Yu, F. Qian, F. Chu, F. Bentzien, B. Cancilla, J. Orf, A. You, A.D. Laird, S. Engst, L. Lee, J. Lesch, Y.C. Chou, A.H. Joly, Cabozantinib (XL184), a novel MET and VEGFR2 inhibitor, simultaneously suppresses metastasis, angiogenesis, and tumor growth, *Mol. Cancer Ther.* 10(2011) 2298-2308.
- [10] Y. Dai, D.W. Siemann, BMS-777607, a small-molecule met kinase inhibitor, suppresses hepatocyte growth factor-stimulated prostate cancer metastatic phenotype *in vitro*, *Mol. Cancer Ther.* 9 (2010) 1554-1561.
- [11] Z. W. Cai, R. M. Borzilleri, 4-pyridinone compounds and their use for cancer, WO2009094417 [P]. 2009-07-30.
- [12] F. Qian, S. Engst, K. Yamaguchi, P. Yu, K.A. Won, L. Mock, T. Lou, J. Tan, C. Li, D. Tam, J. Lougheed, F.M. Yakes, F. Bentzien, W. Xu, T. Zaks, R. Wooster, J. Greshock, A.H. Joly, Inhibition of tumor cell growth, invasion, and metastasis by EXEL-2880 (XL880, GSK1363089), a novel inhibitor of HGF and VEGF receptor tyrosine kinases, *Cancer Res.* 69 (2009) 8009-8016.
- [13] J.K. Rho, Y.J. Choi, S.Y. Kim, T.W. Kim, E.K. Choi, S.J. Yoon, B.M. Park, E. Park, J.H. Bae, C.M. Choi, J.C. Lee, MET and AXL Inhibitor NPS-1034 Exerts Efficacy against Lung Cancer Cells Resistant to EGFR Kinase Inhibitors Because of MET or AXL Activation, *Cancer Res.* 74(2014) 253-262.
- [14] Z. Zhan, J. Ai, Q. Liu, Y. Ji, T. Chen, Y. Xu, M. Geng, W. Duan, Discovery of anilopyrimidines as dual inhibitors of c-Met and VEGFR-2: synthesis, SAR, and cellular activity, *ACS Med. Chem. Lett.* 5 (2014) 673-678.
- [15] S. Zhao, Y. Zhang, H. Zhou, S. Xi, B. Zou, G. Bao, L. Wang, J. Wang, T. Zeng, P. Gong, X. Zhai, Synthesis and biological evaluation of 4-(2-fluorophenoxy)-3,30-bipyridine derivatives as potential c-Met inhibitors, *Eur. J. Med. Chem.* 120 (2016) 37-50,
- [16] W. Gu, Y. Dai, H. Qiang, W. Shi, C. Liao, F. Zhao, W. Huang, H. Qian, Discovery of novel 2-substituted-4-(2-fluorophenoxy) pyridine derivatives possessing pyrazolone and triazole moieties as dual c-Met/VEGFR-2 receptor tyrosine kinase inhibitors, *Bioorg. Chem.* 72 (2017) 116-122.
- [17] Y. Zhao, J. Zhang, R. Zhuang, R. He, J. Xi, X. Pan, Y. Shao, J. Pan, J. Sun, Z. Cai, S. Liu, W. Huang, X. Lv, Synthesis and evaluation of a series of pyridine and pyrimidine derivatives as type II c-Met inhibitors, *Bioorg. Med. Chem.* 25 (2017) 3195-3205,
- [18] N. She, L. Zhuo, W. Jiang, X. Zhu, J. Wang, Z. Ming, X. Zhao, X. Cong, W. Huang, Design, synthesis and evaluation of highly selective pyridone-based class II MET inhibitors, *Bioorg. Med. Chem. Lett.* 24 (2014) 3351-3355.
- [19] J. Liu, M.H. Nie, Y.J. Wang, J.X. Hu, F. Zhang, Y.L. Gao, Y.J. Liu, P. Gong, Design, synthesis and structure-activity relationships of novel 4-phenoxyquinoline derivatives containing 1,2,4-triazolone moiety as c-Met kinase inhibitors, *Euro. J. Med. Chem.* 123 (2016) 431-446.
- [20] S. Li, Q. Huang, Y.J. Liu, X. Zhang, S. Liu, C. He, P. Gong, Design, synthesis and antitumor activity of bisquinoline derivatives connected by 4-oxy-3-fluoroaniline moiety, *Euro. J. Med. Chem.* 64 (2013) 62-73.
- [21] J. Liu, D. Yang, Yang X.X., M.H. Nie, G. Wu, Z. Wang, W. Li, Y.J. Liu, P. Gong, Design, synthesis and biological evaluation of novel 4-phenoxyquinoline derivatives containing 3-oxo-3,4-dihydroquinoxaline moiety as c-Met kinase inhibitors, *Bioorg. Med. Chem.* 25 (2017) 4475-4486.
- [22] S.G. Zhou, H. Liao, C. He, Y. Dou, M. Jiang, L.L. Ren, Y. F. Zhao, P. Gong, Design, synthesis and structure-activity relationships of novel 4-phenoxyquinoline derivatives containing pyridazinone moiety as potential antitumor agents, *Euro. J. Med. Chem.* 83 (2014) 581-593
- [23] Q.D. Tang, L.X. Wang, Y.L. Duan, W.H. Wang, S.M. Huang, J. Zhi, S. Jia, W.F. Zhu, P. Wang, R. Rong, P.W. Zheng, Discovery of novel 7-azaindole derivatives bearing dihydropyridazine moiety as c-Met kinase inhibitors, *Eur. J. Med. Chem.* 133 (2017) 97-106.
- [24] J. Liu, Y.T. Liu, X.C. Hao, Y. Wang, J.C. Ji, Y.J. Liu, S. Ding, Y. Chen, Design, synthesis and biological evaluation of novel 4-phenoxy pyridine derivatives as potential antitumor agents, *Arch. Pharm (Weinheim)*. 352 (2019) e1800338.
- [25] H. Xu, Preparation of quinoline compounds containing 1,2,4-triazine-dione and use as c-Met kinase inhibitors for treating proliferative diseases, US2013/0252958 A1
- [26] D. Katz, E. Ito, K.S. Lau, J.D. Mocanu, C. Bastianutto, A.D. Schimmer, F.F. Liu, Increased efficiency for performing colony

- formation assays in 96-well plates: novel applications to combination therapies and high-throughput screening, *Biotechniques* (2008) 44 (ix-xiv).
- [27] R.L. Vinall, C.G. Tepper, X.B. Shi, L.A. Xue, R. Gandour-Edwards, R.W. deVere White, The R273H p53 mutation can facilitate the androgen-independent growth of LNCaP by a mechanism that involves H2 relaxin and its cognate receptor LGR7, *Oncogene* 25 (2006) 2082-2093.
- [28] S. Shrivastava, M.K. Jeengar, V.S. Reddy, G.B. Reddy, V.G.M. Naidu, Anticancer effect of celastrol on human triple negative breast cancer: possible involvement of oxidative stress, mitochondrial dysfunction, apoptosis and PI3K/Akt pathways, *Exp. Mol. Pathol.* 98 (2015) 313-327.
- [29] S. Shrivastava, P. Kulkarni, D. Thummuri, M.K. Jeengar, V.G.M. Naidu, M. Alvala, G.B. Reddy, S. Ramakrishna, Piperlongumine, an alkaloid causes inhibition of PI3K/Akt/mTOR signaling axis to induce caspase-dependent apoptosis in human triple-negative breast cancer cells, *Apoptosis*.19 (2014) 1148-1164.
- [30] A. Kamal, V. Srinivasulu, V.L. Nayak, M. Sathish, N. Shankaraiah, C. Bagul, N.V.S. Reddy, N. Rangaraj, N. Nagesh, Design and synthesis of C3-pyrazole/chalcone linked b-carboline hybrids: antitopoisomerase I, DNA interactive and apoptosis inducing anticancer agents, *ChemMedChem* 9 (2014) 2084-2098.
- [31] L.G. Rodriguez, X. Wu, J.L. Guan, Wound-healing assay, *Meth. Mol. Biol.* 294 (2005) 23-29.
- [32] D. Katz, E. Ito, K.S. Lau, J.D. Mocanu, C. Bastianutto, A.D. Schimmer, F.F. Liu, Increased efficiency for performing colony formation assays in 96-well plates: novel applications to combination therapies and high-throughput screening, *Biotechniques*. 44 (2008) (ix-xiv).

Legends

Fig. 1. The representative c-Met kinase inhibitors and the corresponding general structure.

Fig. 2. Design strategy and structures of the target compounds.

Scheme 1. Reagents and conditions: (i) cyclopropanecarbonyl chloride, Et₃N, CH₂Cl₂, rt, 12 h; (ii) 2-fluoro-4-nitrophenol, chlorobenzene, reflux, 40 h; (iii) Fe (powder), HOAc, ethyl acetate /water (5:1 v/v), reflux, 2 h.

Scheme 2. Reagents and conditions: (i) NaNO₂, HCl, H₂O, 0 °C, 30 min; (ii) Ethyl acetoacetate, AcONa, EtOH, 0-25 °C, 2 h; (iii) Ph₃P=CHCOOEt, PhMe, reflux, 12 h; (iv) NaOH, THF / H₂O, 50 °C, 5 h; (v) **10**, HATU, Et₃N, DMF, rt, 12 h.

Scheme 3. Reagents and conditions: (i) NaNO₂, HCl, H₂O, 0 °C, 30 min; (ii) ethyl 3-oxopentanoate, AcONa, EtOH, 0-25 °C, 2 h; (iii) DMF-DMA, PhMe, reflux, 12 h; (iv) 10% NaOH, 50 °C, 4 h; (v) **10**, HATU, Et₃N, DMF, rt, 12 h.

Scheme 4. Reagents and conditions: (i) NaNO₂, HCl, H₂O, 0 °C, 30 min; (ii) ethyl (2-cyanoacetyl)carbamate, AcONa, EtOH, 0 °C, 2 h; (iii) HOAc, AcONa, reflux, 2 h; (iv) NaH, CH₃I, DMF, 0 °C, then rt, 5 h; (v) HOAc, HCl, H₂O, reflux, 4 h; (vi) **10**, HATU, Et₃N, DMF, rt, 12 h.

Table 1 Cytotoxicity of target compounds against A549, H460 and HT-29 cells and c-Met kinase inhibition *in vitro*.

Fig. 3. Various concentrations of compound **26a** inhibited colony formation of HT-29 cells for 7 days.

Fig. 4. AO/EB stained apoptosis of HT-29 cell lines with different concentrations of compound **26a** for 48 h.

Fig. 5. Compound **26a** induces cell apoptosis of HT-29 and A549 cell line *in vitro*.

Fig. 6. Effect of compound **26a** *in vitro* migration potential of A549 cells.

Fig. 7. Binding poses of compound **26a** with c-Met (A); 2D interactions of the docking model of **26a** to c-Met (B)

- Three series of novel 4-phenoxy pyridine derivatives were designed and synthesized.
- The target compounds showed c-Met kinase activities and cytotoxic activities
- Compound **26a** showed an IC₅₀ value of 0.016 μM against c-Met kinase.
- The cytotoxic activities of **26a** were more potent than foretinib against H460 and HT-29 cells.
- Compound **26a** could suppress the colony formation, induce cells apoptosis and inhibit cells motility.

Journal Pre-proof

Declaration of interests

The authors declare that they have no known competing financial interests or personal relationships that could have appeared to influence the work reported in this paper.

Journal Pre-proof